

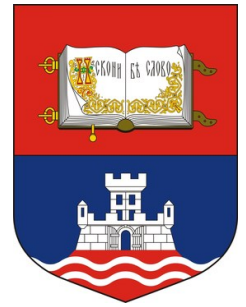


УНИВЕРЗИТЕТ У БЕОГРАДУ
ИНСТИТУТ ЗА ФИЗИКУ | БЕОГРАД
ИНСТИТУТ ОД НАЦИОНАЛНОГ
ЗНАЧАЈА ЗА РЕПУБЛИКУ СРБИЈУ



2019 COST Action THOR Annual Meeting

2-6 September 2019
Istanbul Technical University
Europe/Istanbul timezone



Dynamical energy loss formalism and constraining the initial stages with high- p_{\perp} observables

Bojana Ilic (Blagojevic)

Institute of Physics Belgrade

University of Belgrade

Motivation

- Energy loss of high- p_{\perp} particles traversing QCD medium is an excellent probe of QGP properties.
- Theoretical predictions can be compared with a wide range of data, coming from different experiments, collision systems, collision energies, centralities, observables...
- Can be used together with low- p_{\perp} theory and experiments to study the properties of created QCD medium, i.e. for precision QGP tomography.

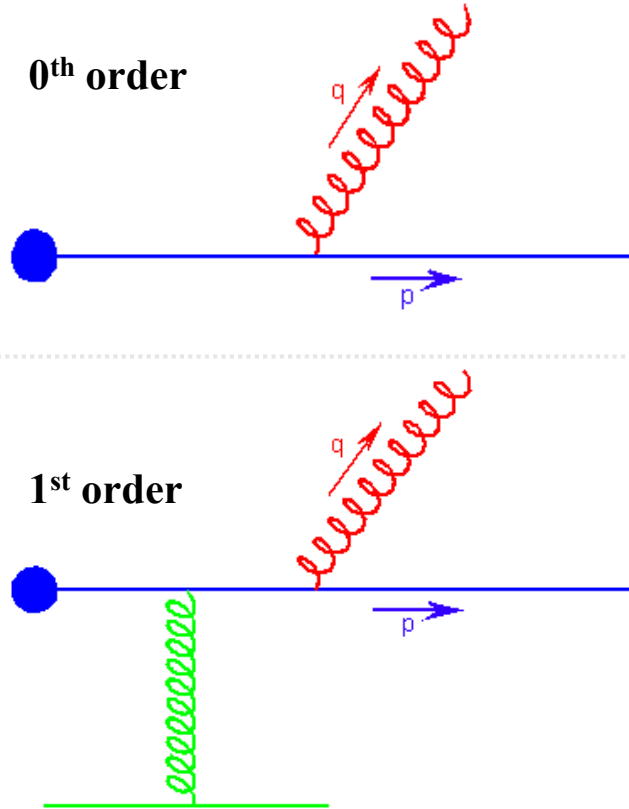
Outline

- ✓ Dynamical energy loss formalism (embedded in DREENA framework)
 - Beyond soft-gluon approximation
- ✓ Constraining the initial stages before QGP thermalization with high- p_{\perp} theory and data

Dynamical energy loss formalism

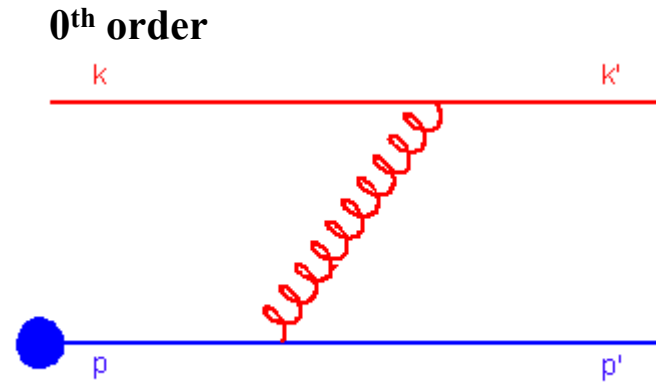
Radiative energy loss

Radiative energy loss comes from the processes in which there are more outgoing than incoming particles:



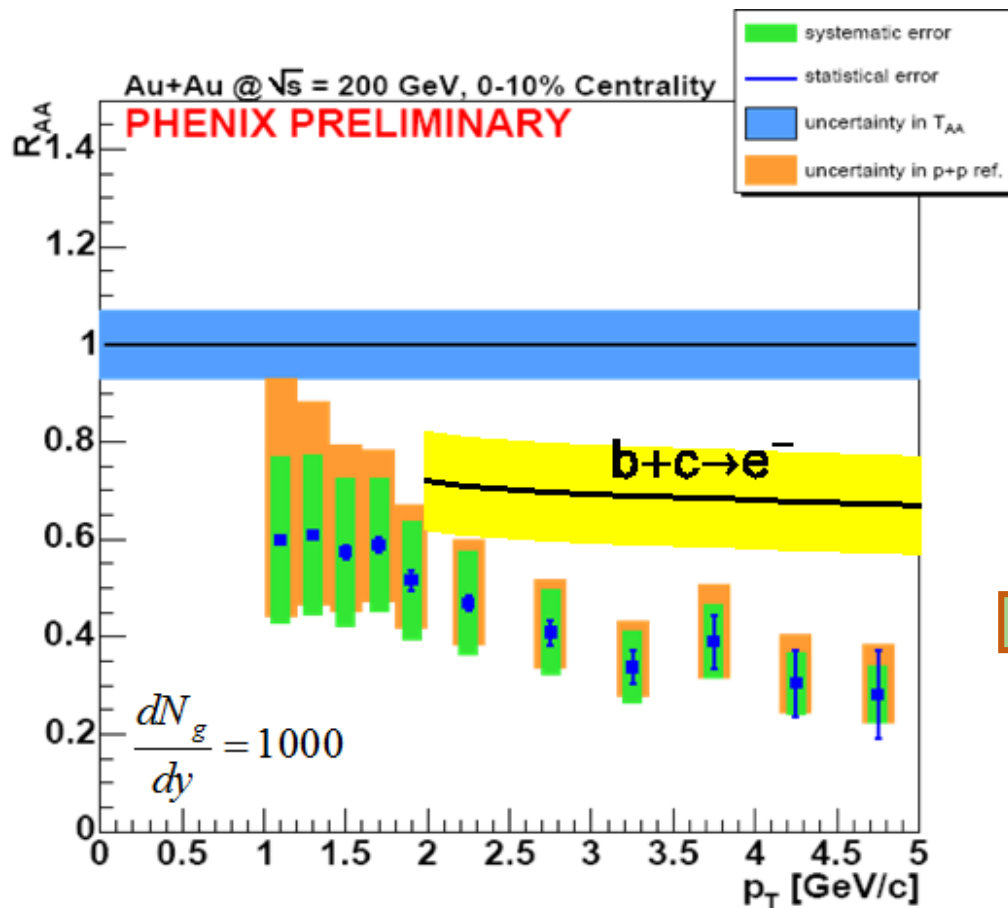
Collisional energy loss

Collisional (elastic) energy loss comes from the processes which have the same number of incoming and outgoing particles:



Single electron puzzle at RHIC

M. Djordjevic, M. Gyulassy, R. Vogt and S. Wicks, PLB 632, 81 (2006).



DGLV

Radiative energy loss
in medium consisting
of **static** scattering
centers.

M. Djordjevic and M. Gyulassy, NPA 733, 265 (2004).

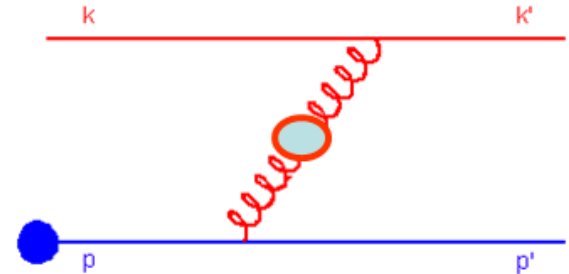
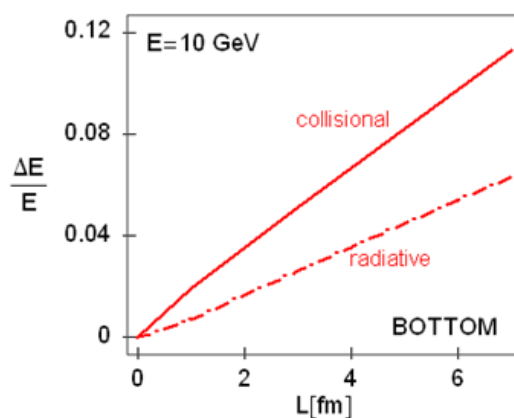
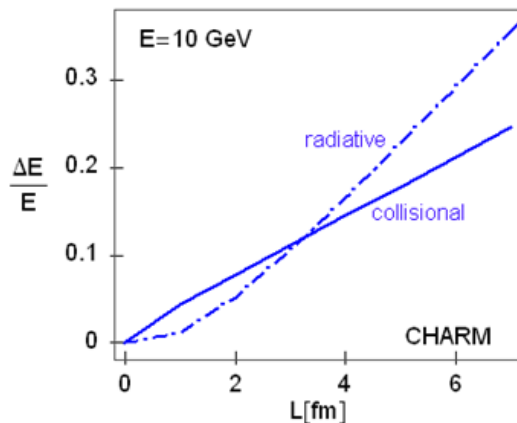
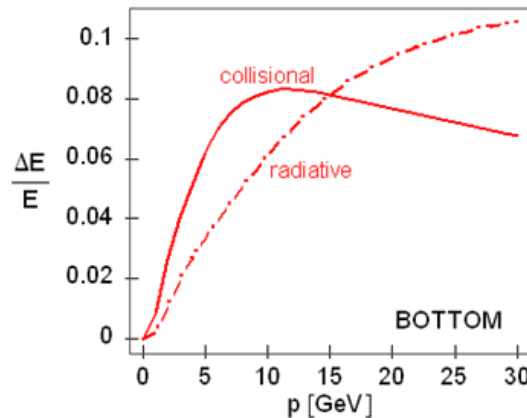
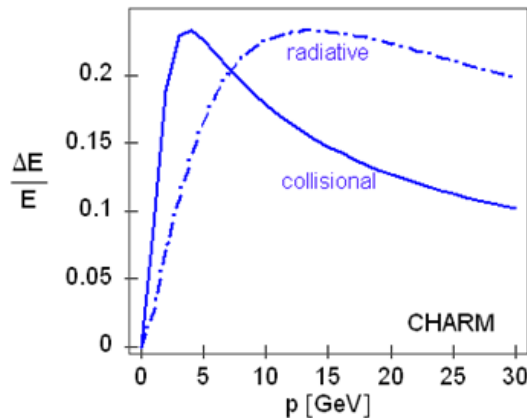
Inconsistent!

Radiative energy loss
alone is insufficient to
explain the single
electron R_{AA} data.

Collisional energy loss

- Collisional energy loss in a finite size QCD medium of temperature T

(1-HTL) M. Djordjevic, PRC 74,064907 (2006).



Collisional and
radiative energy
losses are
comparable!



Collisional energy loss
has to be also included.

Radiative energy loss

Static QCD medium approximation
(modeled by Yukawa potential).

Collisional energy loss

ΔE_{coll} exactly equal to zero!



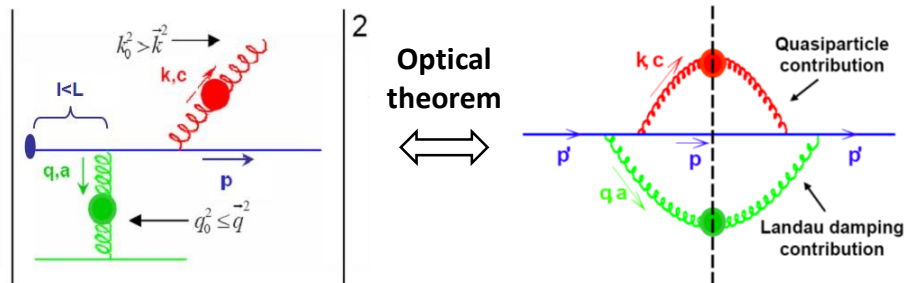
Collisional and radiative energy
losses are shown to be comparable.

Inclusion of collisional energy loss
is **necessary**, but **inconsistent** with
static approximation!

QGP medium consisting of **dynamical scatterers**, and not
static, **has to** be used in **radiative energy loss** calculations,
as well!

Radiative energy loss in dynamical medium

✓ We assume:



- Dynamical medium of a finite size L , consisting of thermally distributed massless partons
- 1st order in opacity (two Hard-Thermal Loop approach)

M. Djordjevic, PRC 80,064909 (2009) (highlighted in APS physics),

M. Djordjevic and U. Heinz, PRL 101,022302 (2008).

- **Radiated gluon**: transversely polarized with effective mass given by $m_g = \mu_E/\sqrt{2}$

M.Djordjevic and M. Gyulassy, PRC 68, 034914 (2003).

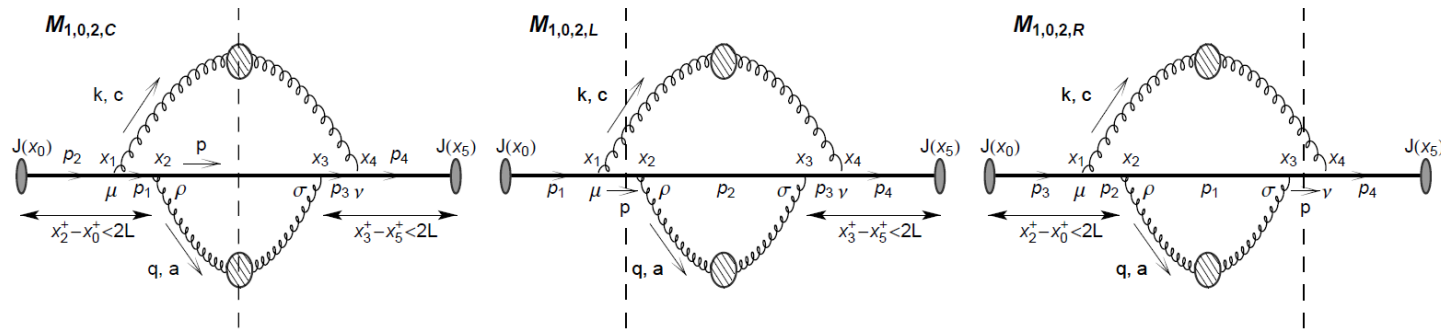
- **Exchanged gluon** cut 1-HTL propagator retains both transverse (magnetic) and longitudinal (electric) parts.

Radiative energy loss in dynamical medium

In finite size dynamical QGP medium produced quark can be both **on-** and **off-shell**.



Beside central cut, left and right cuts are allowed.



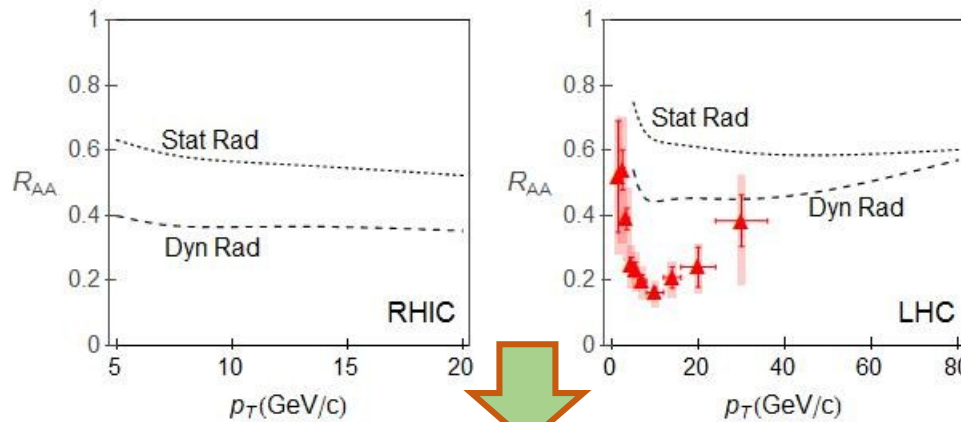
All 24 relevant diagrams are calculated. Each of them is infrared divergent, due to the absence of magnetic screening.



The divergence is naturally regulated when all the diagrams are taken into account.

$$\frac{\Delta E_{dyn}}{E} = \frac{C_R \alpha_s}{\pi} \frac{L}{\lambda_{dyn}} \int dx \int \frac{d^2 q_l}{\pi} \frac{\mu_E^2}{q_l^2 (q_l^2 + \mu_E^2)} \int dk^2 \frac{2}{(k - q_l)^2 + \chi} \left(1 - \frac{\sin\left(\frac{(k - q_l)^2 + \chi}{2xE} L\right)}{\frac{(k - q_l)^2 + \chi}{2xE}} \right) \left(\frac{(k - q_l)^2}{(k - q_l)^2 + \chi} - \frac{k \cdot (k - q_l)}{k^2 + \chi} \right)$$

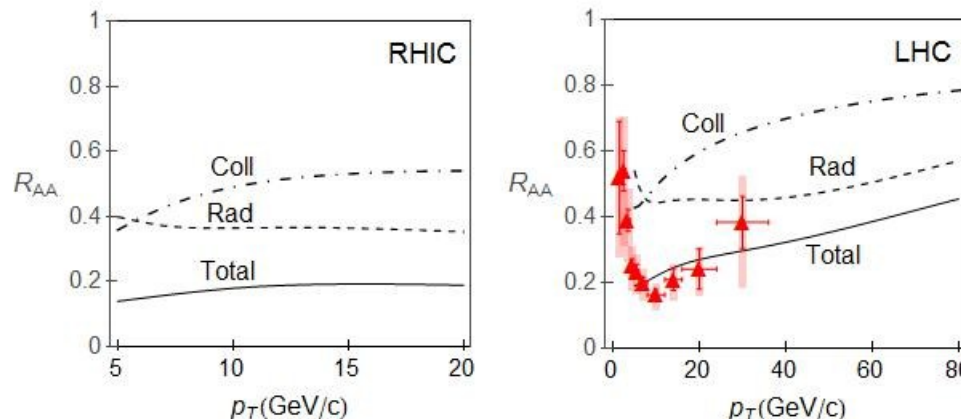
The importance of dynamical effects



NPA 904-905, 635c (2013) ;
JHEP 1209,112 (2012) .

Dynamical effects in radiative part lead to a **significant suppression increase**.

Dynamical effects in radiative part alone are **important**, but **insufficient**.



**Collisional + radiative
energy losses computed
within the same
(dynamical) theoretical
framework
lead to a good
agreement with data!**

B. Blagojevic and M. Djordjevic, JPG 42, 075105 (2015) (highlighted in LabTalk).

Dynamical energy loss formalism

- Finite T, finite size medium consisting of dynamical partons
- Based on finite T Field Theory and generalized HTL approach

M. Djordjevic, PRC 74, 064907 (2006); PRC 80, 064909 (2009), M. Djordjevic and U. Heinz, PRL 101, 022302 (2008).

- Collisional + radiative energy losses computed within the same theoretical framework
- Finite magnetic mass effect

M. Djordjevic and M. Djordjevic, PLB 709, 229 (2012).

- Running coupling

M. Djordjevic and M. Djordjevic, PLB 734, 286 (2014).

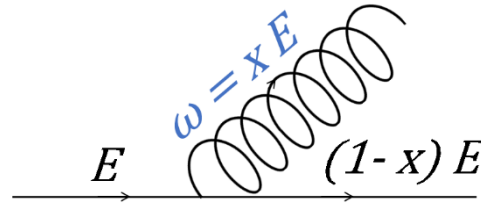
- Relaxed soft-gluon approximation

B. Blagojevic, M. Djordjevic and M. Djordjevic, PRC 99, 024901, (2019).



All ingredients are **important** for accurate description of high- p_{\perp} R_{AA} data!

Relaxing the soft-gluon approximation



- **The soft-gluon approximation (sg) definition** – radiated gluon carries away a small fraction of initial jet energy $x = \frac{\omega}{E} \ll 1$.
- **Widely-used assumption in calculating radiative energy loss of high p_{\perp} particle traversing QGP**

ASW (PRD, 69:114003), BDMPS (NPB, 484:265), BDMPS-Z (JETP Lett., 65:615), GLV (NPB 594:371), HT (NPA 696:788);

M. Djordjevic, PRC , 80:064909 (2009), M. Djorjevic and U. Heinz, PRL, 101:022302 (2008).

Why do we reconsider the soft-gluon approximation validity?

- **Significant** medium induced **radiative energy loss** obtained by different models → **inconsistent** with **sg** approximation?
- Sg approximation also used in our **Dynamical energy loss formalism**.

M. Djordjevic and M. D. PLB 734:286 (2014).

- Our dynamical energy loss model reported robust agreement with extensive set of experimental R_{AA} data → implies model **reliability**.

M. Djordjevic and M. D. PLB 734:286 (2014), PRC 90:034910 (2014),

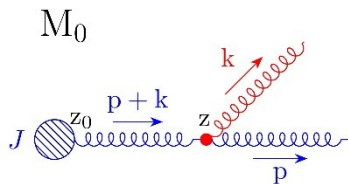
M. Djordjevic, M. D. and B. Blagojevic PLB 737:298 (2014); M. Djordjevic PRL 112:042302 (2014)

M. Djordjevic and M. D. PRC 92:024918 (2015).

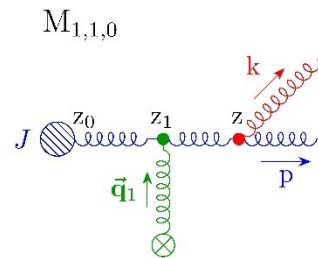
- It **breaks-down** for:
 - $5 < p_{\perp} < 10$ GeV
 - Primarily for gluon energy loss

Calculations beyond soft-gluon approximation

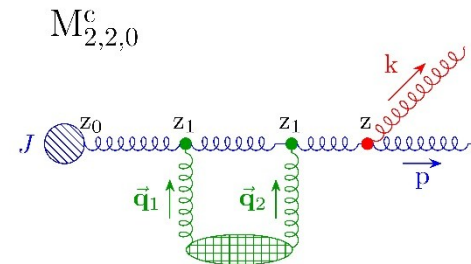
0th order



Interaction with one scatterer



Interaction with two scatterers in contact limit



□ Beyond soft-gluon approximation (***bsg***) in DGLV:
 x finite

□ Assumptions:

- Initial gluon propagates along the longitudinal axis
- The soft-rescattering (eikonal) approximation
- The 1st order in opacity approximation

M. Gyulassy, P. Levai and I. Vitev, PLB 538:282 (2002).

B. Blagojevic, M. Djordjevic and M. Djordjevic, PRC 99, 024901, (2019).

Comparison of analytical expressions $\left(\frac{dN_g^{(1)}}{dx}\right)$

Beyond soft-gluon approximation:

$$f_{\text{bsg}}(\mathbf{k}, \mathbf{q}_1, x) = \frac{(1-x+x^2)^2}{x(1-x)} \left\{ \left(2 \frac{(\mathbf{k} - \mathbf{q}_1)^2}{(\mathbf{k} - \mathbf{q}_1)^2 + \chi} - \frac{\mathbf{k} \cdot (\mathbf{k} - \mathbf{q}_1)}{\mathbf{k}^2 + \chi} - \frac{(\mathbf{k} - \mathbf{q}_1) \cdot (\mathbf{k} - x\mathbf{q}_1)}{(\mathbf{k} - x\mathbf{q}_1)^2 + \chi} \right) \frac{(\mathbf{k} - \mathbf{q}_1)^2 + \chi}{\left(\frac{4x(1-x)E}{L} \right)^2 + ((\mathbf{k} - \mathbf{q}_1)^2 + \chi)^2} \right. \\ \left. + \frac{\mathbf{k}^2 + \chi}{\left(\frac{4x(1-x)E}{L} \right)^2 + (\mathbf{k}^2 + \chi)^2} \left(\frac{\mathbf{k}^2}{\mathbf{k}^2 + \chi} - \frac{\mathbf{k} \cdot (\mathbf{k} - x\mathbf{q}_1)}{(\mathbf{k} - x\mathbf{q}_1)^2 + \chi} \right) + \left(\frac{(\mathbf{k} - x\mathbf{q}_1)^2}{((\mathbf{k} - x\mathbf{q}_1)^2 + \chi)^2} - \frac{\mathbf{k}^2}{(\mathbf{k}^2 + \chi)^2} \right) \right\}$$

$$\chi = m_g^2(1 - x + x^2)$$

Soft-gluon approximation:

$$f_{\text{sg}}(\mathbf{k}, \mathbf{q}_1, x) = \frac{1}{x} \frac{(\mathbf{k} - \mathbf{q}_1)^2 + m_g^2}{\left(\frac{4xE}{L} \right)^2 + ((\mathbf{k} - \mathbf{q}_1)^2 + m_g^2)^2} 2 \left(\frac{(\mathbf{k} - \mathbf{q}_1)^2}{(\mathbf{k} - \mathbf{q}_1)^2 + m_g^2} - \frac{\mathbf{k} \cdot (\mathbf{k} - \mathbf{q}_1)}{\mathbf{k}^2 + m_g^2} \right)$$

M. Djordjevic and M. Gyulassy, NPA 733:265(2004).

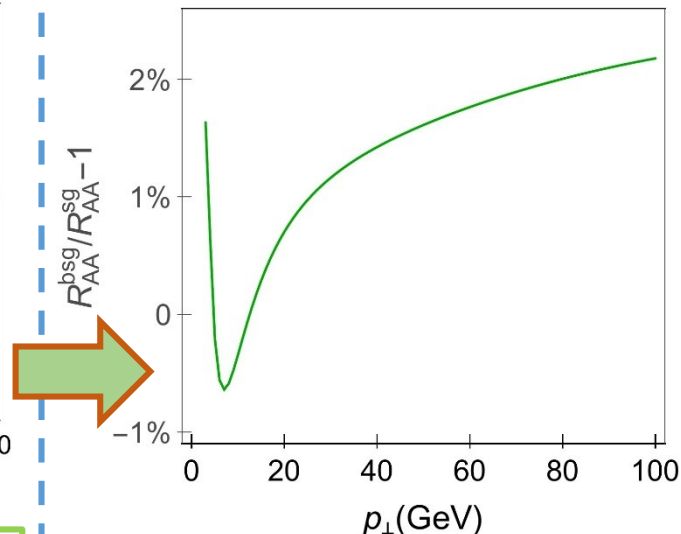
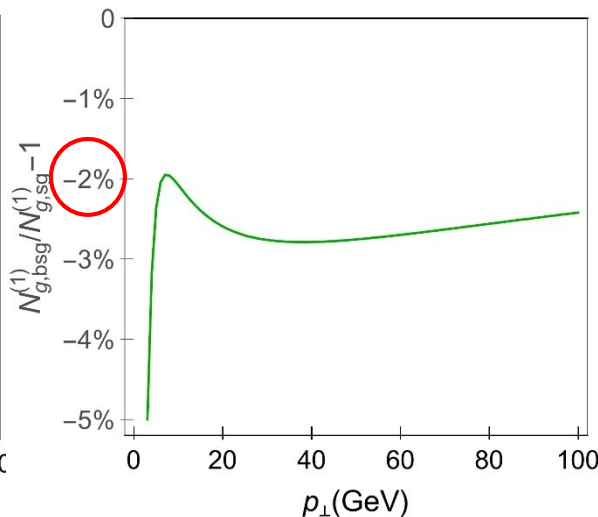
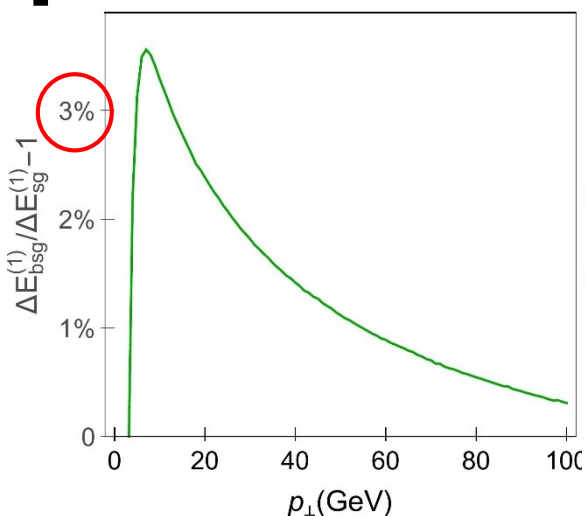
Only this
term
remains in
sg and
reduces to:

B. Blagojevic, M. Djordjevic
and M. Djordjevic, PRC 99,
024901, (2019).

Bsg expression is quite
different and **notably more**
complex than its *sg*
analogon!



Effect of relaxing *sga* on numerical predictions



Slightly **increased**
 $\frac{\Delta E}{E}$ compared to *sg*.

Slightly **decreased**
 N_g compared to *sg*.

R_{AA} **negligibly**
affected!

Effect on $\Delta E^{(1)} / E$ and $N_g^{(1)}$
is **very small** and of an **opposite**
sign, and they both non-trivially
affect R_{AA} !

Interplay of the
opposite effects on
 $\Delta E^{(1)} / E$ and $N_g^{(1)}$ is
responsible for
negligible effect on
 R_{AA} .

Conclusion for this part

Different theoretical models reported considerable radiative energy loss questioning the validity of the soft-gluon approximation.

We relaxed the approximation for **high p_{\perp} gluons**, which are most affected by it, within **DGLV** formalism, and although analytical results are very different in **bsg** and **sg** cases, surprisingly the numerical predictions were nearly indistinguishable.

Consequently, this relaxation should have even smaller impact on high p_{\perp} quarks.

This implies that soft gluon approximation is reliable within DGLV formalism

Based on our previous analysis we expect that the soft-gluon approximation remains well-founded within the dynamical energy loss formalism as well.

DREENA-B framework

- **DREENA-B (Dynamical Radiative and Elastic ENergy loss Approach + Bjorken expansion) framework** presents fully optimized numerical suppression procedure, based on:

D. Zigic, I. Salom, M. Djordjevic and M. Djordjevic, PLB 791, 236 (2019).

- **Dynamical energy loss formalism**
- **Medium evolution introduced through 1+1D Bjorken expansion**

J. D. Bjorken, PRD 27, 140 (1983).

Assessing the features of Initial Stages (IS)

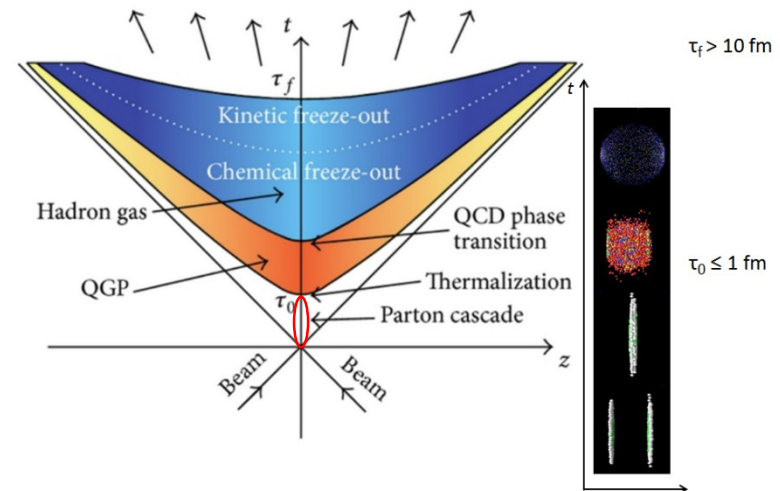
- Traditionally, rare **high- p_{\perp} probes** ($p_{\perp} \geq 5$ GeV) are utilized for studying the nature of jet-medium interactions.
- Commonly, **low- p_{\perp} sector** ($p_{\perp} \leq 5$ GeV) is used to infer the features of **initial stages before the QGP thermalization**

F. Gelis and B. Schenke, ARNPS 66, 73 (2016);

G. Aad et al. [ATLAS Collaboration], JHEP 1311, 183 (2013);

H. Niemi, G. S. Denicol, H. Holopainen and P. Huovinen, PRC 87, 054901 (2013).

- IS properties poorly-known up-to-date



High- p_{\perp} observables as a novel tool for IS studies

- **High p_{\perp} partons effectively probe** QGP properties, which in turn depend on initial QGP stages
- **Recently a wealth of high- p_{\perp} experimental data became available**

JHEP 1811, 013; JHEP 1704, 039; ATLAS-CONF-2017-012; JHEP 1807, 103; PLB 776, 195; EPJC 78, 997; PRL 120, 102301; PRL 120, 202301.

- **Current theoretical studies on this subject are either inconclusive or questionable** – e.g. the energy loss parameters were fitted to reproduce experimental RAA data, individually for different analyzed T profiles.

J. Xu, A. Buzzatti and M. Gyulassy, JHEP 1408, 063 (2014);

C. Andres, N. Armesto, H. Niemi, R. Paatelainen and C. A. Salgado, arXiv:1902.03231 (2019);

R. Katz, C. A. G. Prado, J. Noronha-Hostler, J. Noronha and A. A. P. Suaide, arXiv:1906.10768 (2019).

Our approach

✓ For higher control over the **energy loss** and **IS** we employ full-fledged **DREENA-B framework**, because:

□ Bjorken 1+1D:

- Allows analytical introduction of different evolutions before, and the same evolution after thermalization
- Facilitates the isolation of IS effects alone
- Presents a reasonable description of medium evolution (compared to 3+1D hydrodynamical evolution)
(the next talk by Dusan Zigic)

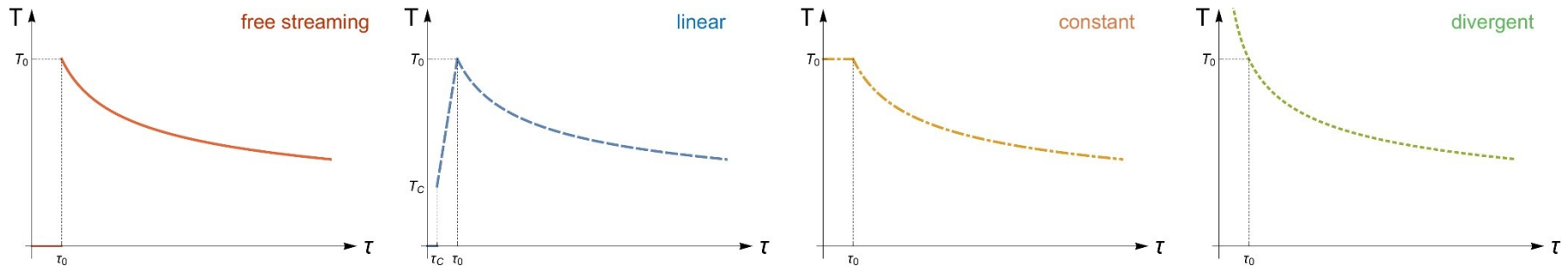
□ Dynamical energy loss formalism:

- Complex, enclosing some unique realistic features
- Dominant ingredient for generating high- p_{\perp} predictions

D. Zigic, B. Ilic, M. Djordjevic and M. Djordjevic, arXiv:1908.11866.

Four common cases of Initial Stages (IS)

J. Xu, A. Buzzatti and M. Gyulassy, JHEP 1408, 063 (2014).



✓ Initial-stage cases have the same 1+1D Bjorken T profile upon thermalization, but differ for $\tau < \tau_0 = 0.6$ fm:

a) *Free streaming*, $T = 0$

b) *Linear*, linearly increasing T from $T_C = 160$ MeV to $T_0 = 391$

MeV (30-40 %, 5.02 TeV *Pb+Pb*)

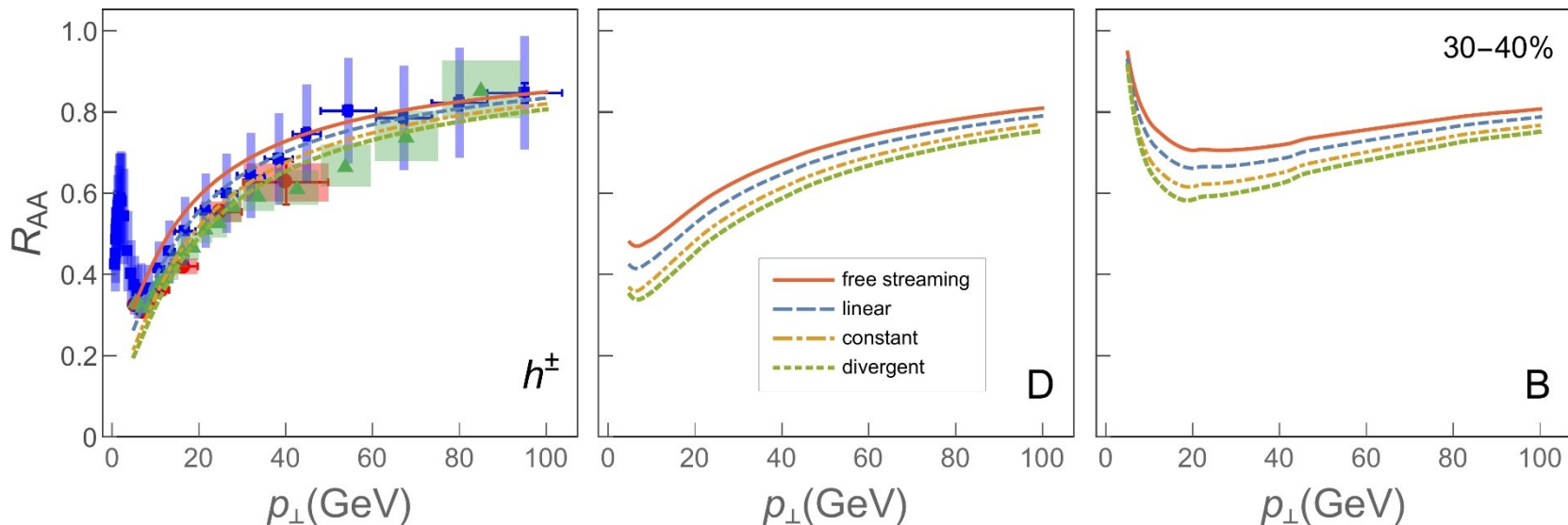
D. Zigic, I. Salom, M. Djordjevic and
M. Djordjevic, PLB 791, 236 (2019)

c) *Constant*, $T = T_0$

d) *Divergent*, Bjorken expansion from $\tau = 0$

D. Zigic, B. Ilic, M. Djordjevic and M. Djordjevic, arXiv:1908.11866.

Sensitivity of high- p_{\perp} R_{AA} to the IS



ALICE: JHEP 1811, 013 (2018);
ATLAS-CONF-2017-012;
CMS: JHEP 1704, 039 (2017).

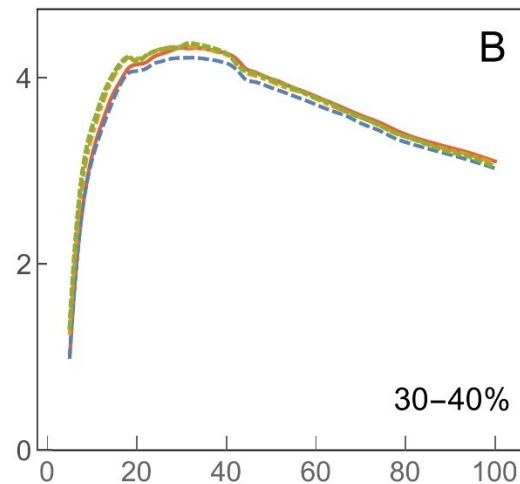
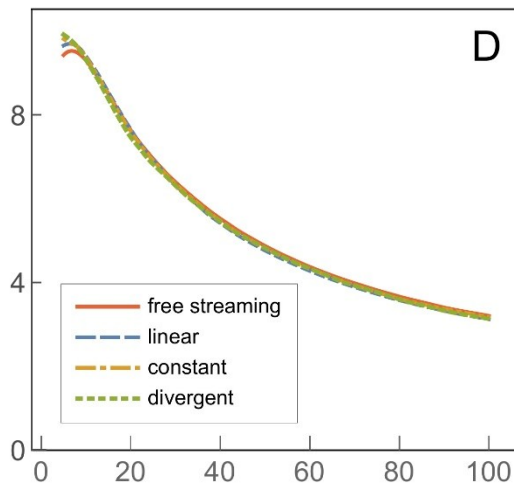
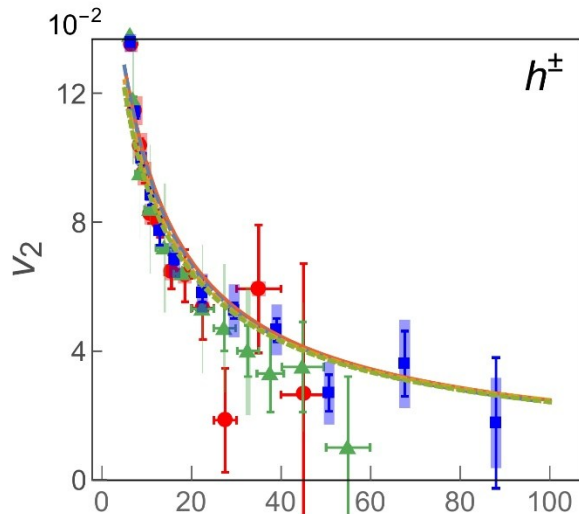
D. Zigic, B. Ilic, M. Djordjevic and M. Djordjevic, in preparation

High- p_{\perp} R_{AA} is **notably affected** by the presumed initial stages, due to difference in energy loss.

However, current error-bars at the LHC do not allow distinguishing between these cases.

Sensitivity of high- p_{\perp} v_2 to the IS

!



ALICE: JHEP 1807, 103 (2018);
ATLAS: EPJC 78, 997 (2018);
CMS: PLB 776, 195 (2018).



v_2 is practically insensitive to the initial stages.



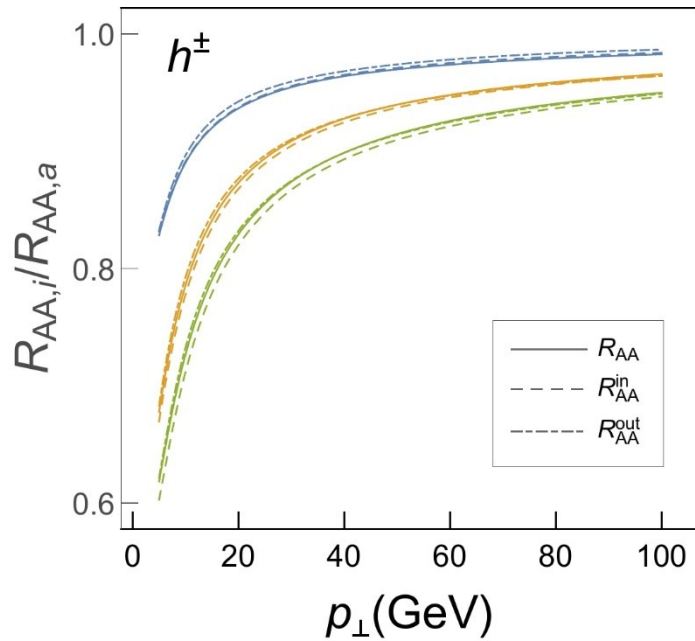
C. Andres, N. Armesto, H. Niemi, R. Paatelainen
and C. A. Salgado, arXiv:1902.03231.



High- p_{\perp} v_2 cannot distinguish between different IS scenarios!

D. Zigic, B. Ilic, M. Djordjevic and M. Djordjevic, arXiv:1908.11866.

Explanation of the obtained results



$$R_{AA} \approx \frac{R_{AA}^{in} + R_{AA}^{out}}{2}$$

$$v_2 \approx \frac{1}{2} \frac{R_{AA}^{in} - R_{AA}^{out}}{R_{AA}^{in} + R_{AA}^{out}}$$

- Blue = Linear/Free streaming
 - Orange = Constant/Free streaming
 - Green = Divergent/Free streaming
- Sets of curves

Proportionality functions:

$i = \text{lin, const, div}$

$$\gamma_i = \frac{R_{AA,i}}{R_{AA,fs}}$$

$$\gamma_i^{in} = \frac{R_{AA,i}^{in}}{R_{AA,fs}^{in}}$$

$$\gamma_i^{out} = \frac{R_{AA,i}^{out}}{R_{AA,fs}^{out}}$$

$$\gamma_i^{in} \approx \gamma_i^{out} \approx \gamma_i$$

$$\forall i \in \{\text{Blue, Orange, Green}\}$$

$$\gamma_i < 1$$

$$R_{AA,i} \approx \frac{\gamma_i (R_{AA,fs}^{in} + R_{AA,fs}^{out})}{2} = \gamma_i R_{AA,fs}$$

$$v_{2,i} \approx \frac{1}{2} \frac{\gamma_i (R_{AA,fs}^{in} - R_{AA,fs}^{out})}{\gamma_i (R_{AA,fs}^{in} + R_{AA,fs}^{out})} = v_{2,fs}$$

Explanation of high- p_{\perp} R_{AA} results through analytical estimate

R_{AA} is shown to be sensitive only to the averaged properties of the evolving medium

$$1 - R_{AA} \sim \frac{\Delta E}{E} \sim \bar{T}$$

Analytical estimate, but for all predictions we apply full-fledged numerical calculations!

D. Zigic, I. Salom, M. Djordjevic and M. Djordjevic, PLB 791, 236 (2019);

T. Renk, PRC 85, 044903 (2012);

D. Molnar and D. Sun, NPA 932, 140 (2014); 910-911, 486 (2013).

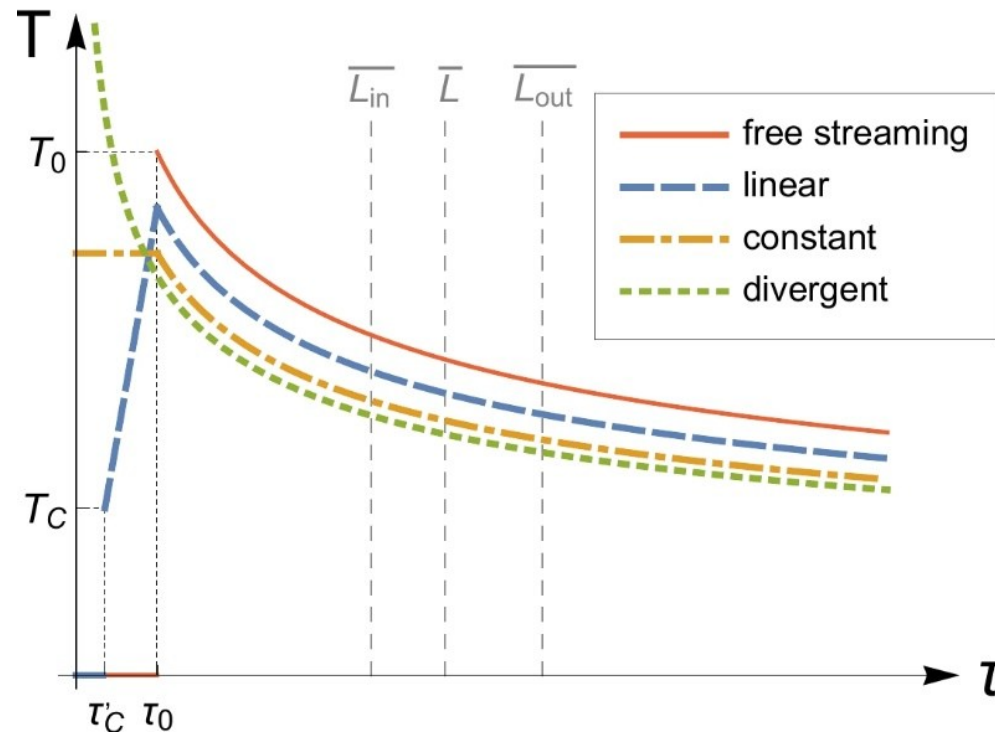


Different \bar{T} s for four IS cases result in different R_{AA} s.



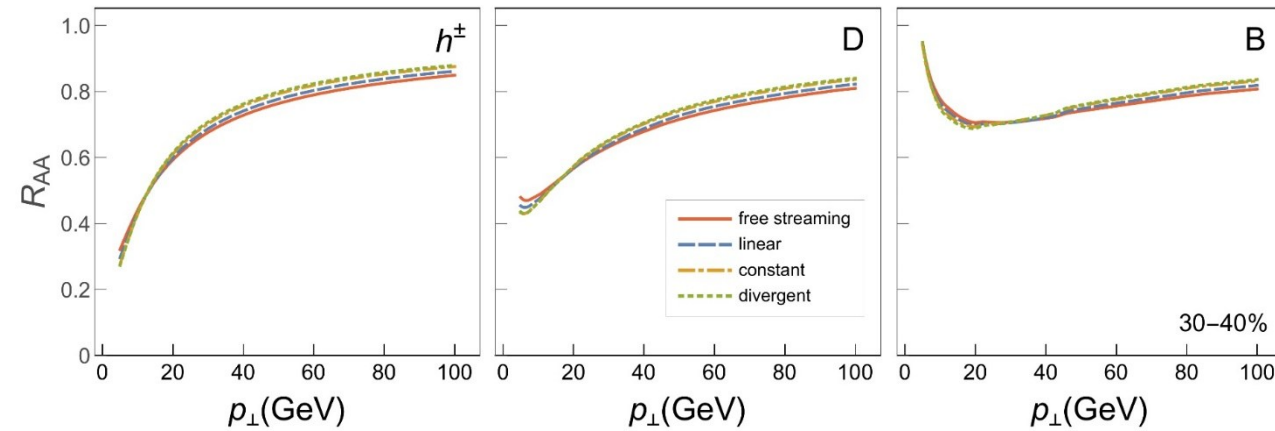
What are the effects of modified T-profile cases, which ensure the same average T?

Modified temperature profiles

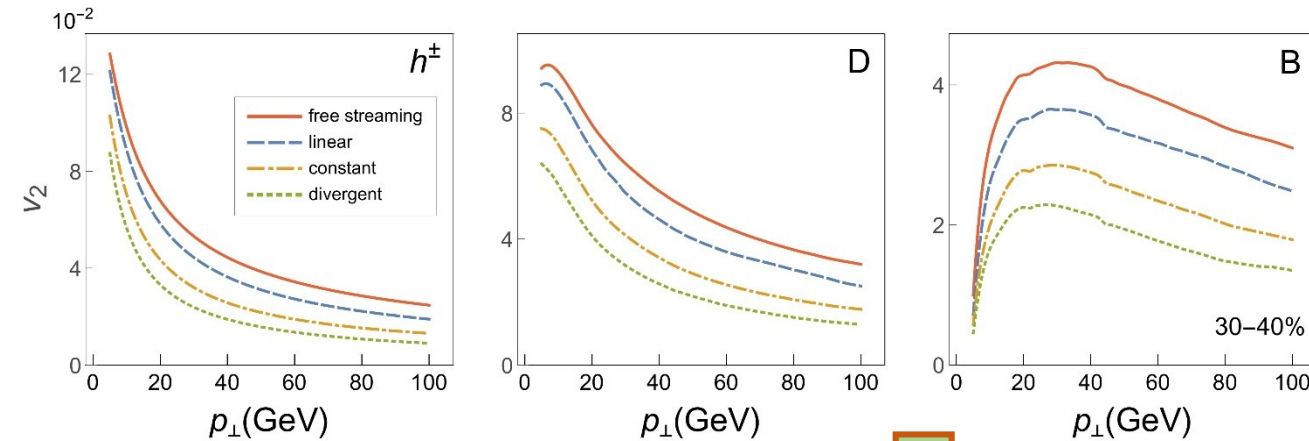


Modified T-profile cases differ not only at initial stages, but represent **different evolutions altogether!**

Sensitivity of high- p_{\perp} v_2 to modified T profiles



The **overlap** of high- p_{\perp} R_{AA} curves in all four modified cases is verified.



High- p_{\perp} v_2 is **very sensitive** to different evolutions.

The highest v_2 is observed in free-streaming case.

Sensitivity of high- p_{\perp} v_2 to modified T profiles

v_2 is **very sensitive** to these different evolutions.



Why is v_2 altered by these modified T-profile cases?



Are the initial stages at the origin of these v_2 discrepancies?

Why is high- p_{\perp} v_2 affected by modified T profiles?

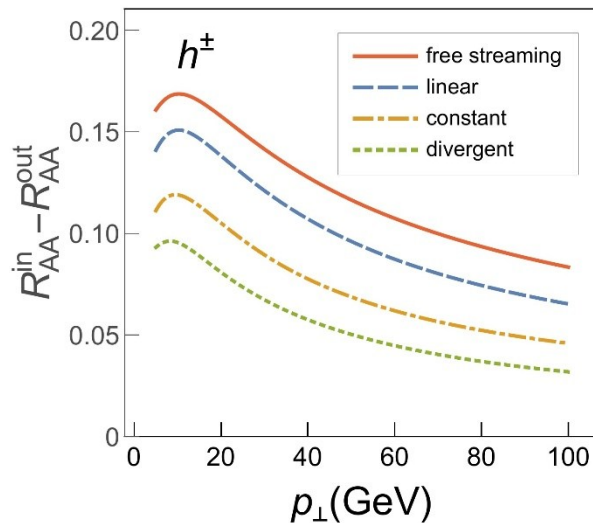
$$v_2 \approx \frac{1}{2} \frac{R_{AA}^{in} - R_{AA}^{out}}{R_{AA}^{in} + R_{AA}^{out}}$$



R_{AA}
practically
unchanged.



$$v_2 \sim R_{AA}^{in} - R_{AA}^{out}$$

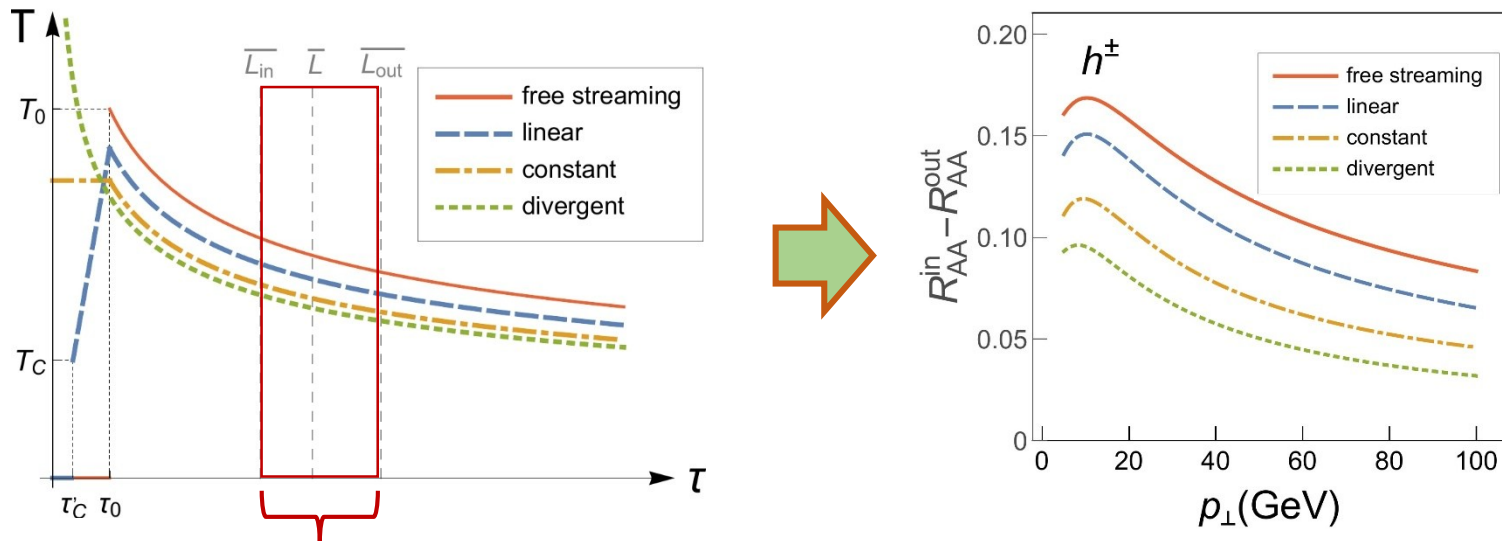


The same curve ordering
as for high- p_{\perp} v_2 .



$R_{AA}^{in} - R_{AA}^{out}$ differences are
responsible for high- p_{\perp} v_2
discrepancies.

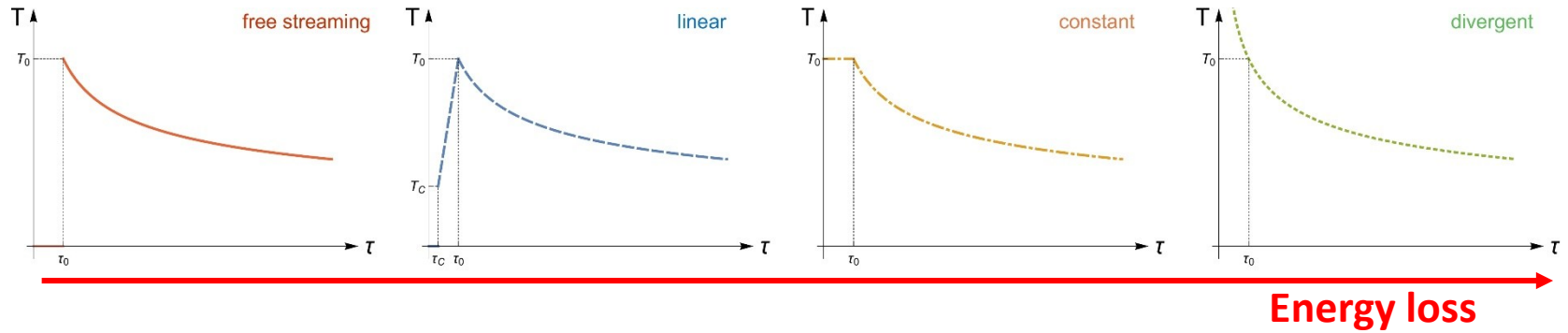
Is IS responsible for high- p_{\perp} v_2 discrepancies?



This region contributes to $R_{AA}^{in} - R_{AA}^{out}$ differences.

Large v_2 sensitivity originates from interactions of high- p_{\perp} parton with *thermalized* QGP, and *not the initial stages*!

Fitting energy loss parameters to high- p_{\perp} R_{AA} experimental data



JHEP 1408, 090 (2014), PRL 116, 252301 (2016), arXiv:1902.03231 (2019), PRC 96, 064903 (2017), PRC 95, 044901 (2017), PRC 96, 024909 (2017).

Fitting the energy loss (**multiplicative fitting factor**), to reproduce the high- p_{\perp} R_{AA} data, individually for different initial stages

An additional fitting factor $C_i^{fit}(p_{\perp})$ is introduced in our full-fledged calculations.

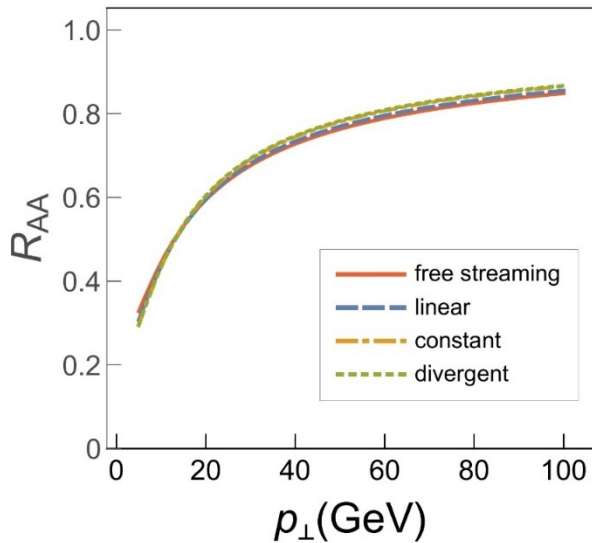


Best fits to $R_{AA,fs}$ yield:

T profile case	C_i^{fit}
Free-streaming case (a)	1
Linear case (b)	0.87
Constant case (c)	0.74
Divergent case (d)	0.67

TABLE I: Fitting factors values

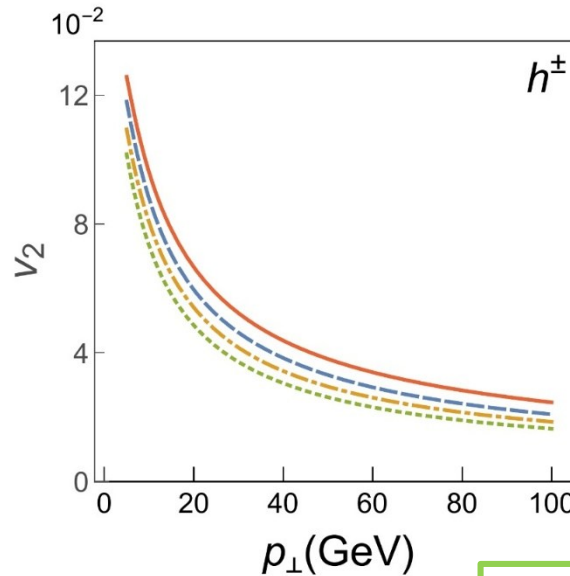
Sensitivity of high- p_{\perp} fitted R_{AA} to IS



High- p_{\perp} R_{AA} s are overlapping.



Inconsistent with our previous analysis and also intuitive expectation that higher energy loss at IS leads to lower R_{AA} !



High- p_{\perp} v_2 is notably affected!



Is this a consequence of initial stages?

C. Andres, N. Armesto, H. Niemi, R. Paatelainen and C. A. Salgado, arXiv:1902.03231 (2019).



Asymptotical scaling behavior

- For quantitative explanation of the obtained results
- Assumptions:
 - Highly energetic jets
 - More peripheral collisions


$$R_{AA} \approx 1 - \xi \bar{T}^a \bar{L}^b$$

D. Zigic, I. Salom, M. Djordjevic and M. Djordjevic, PLB 791, 236 (2019);

M. Djordjevic, D. Zigic, M. Djordjevic and J. Auvinen, PRC 99, 061902 (2019).

$i = \text{lin, const, div}$


$$R_{AA,i}^{fit} \approx 1 - C_i(p_{\perp}) \xi \bar{T}_i^a \bar{L}_i^b$$

$$R_{AA,i}^{fit} = R_{AA,fs}$$


$$v_{2,i}^{fit} = C_i \gamma_i v_{2,fs}$$

$C_i, \gamma_i < 1$ γ_i approaches 1 at very high p_{\perp}

Diminishing of $v_{2,i}$ compared to the *fs* case is predominantly a consequence of a decrease in the **artificially imposed fitting factor**



Fitting energy loss to individual IS may result in **misinterpreting** the underlying physics!

Conclusions

Low- p_{\perp} sector is traditionally used to study the initial stages (IS) before QGP thermalization, but recent acquisition of wealth of high- p_{\perp} experimental data motivated exploiting high- p_{\perp} energy loss in studying the IS.

To this end, we utilized state-of-the-art dynamical energy loss formalism embedded in 1+1D Bjorken medium expansion: **DREENA-B framework**, to assess the effects of four commonly considered IS cases on high- p_{\perp} observables, and obtained that **high- p_{\perp} R_{AA}** is **sensitive** to the presumed IS. However, within the current error bars, the sensitivity is insufficient to distinguish between different initial scenarios.

Unexpectedly, we found that **high- p_{\perp} v_2** is **insensitive** to the IS. Moreover, by combining full-fledged numerical predictions and analytical estimates, we inferred that previously reported sensitivity of high- p_{\perp} v_2 to IS is mostly an artefact of the fitting procedure.

Multiple fitting procedure of energy loss parameter for each individual IS may result in **incorrect** energy loss estimates and in overlooking the underlying physics.

Overall, the **simultaneous study of high- p_{\perp} R_{AA} and v_2** , with **consistent/fixed energy loss parameters across the entire study**, and **controlled temperature profiles**, is crucial for imposing accurate constraints on the initial stages.



European Research Council
Established by the European Commission



МИНИСТАРСТВО ПРОСВЕТЕ,
НАУКЕ И ТЕХНОЛОШКОГ РАЗВОЈА

Thank you for your attention!

In collaboration with: Magdalena Djordjevic, Marko Djordjevic, Pasi Huovinen, Jussi Auvinen, Igor Salom, Dusan Zigic and Stefan Stojku

Backup

Calculations beyond soft-gluon approximation

$$M_0 = J_a(p+k)e^{i(p+k)x_0}(-2ig_s)(1-x+x^2) \times \frac{\epsilon \cdot k}{k^2 + m_g^2(1-x+x^2)}(T^c)_{da}.$$

No interaction with QGP medium

$$M_{1,1,0} = J_a(p+k)e^{i(p+k)x_0}(-i)(1-x+x^2)(T^c T^{a_1})_{da} T_{a_1} \int \frac{d^2 \mathbf{q}_1}{(2\pi)^2} v(0, \mathbf{q}_1) e^{-i\mathbf{q}_1 \cdot \mathbf{b}_1} \times (-2ig_s) \frac{\epsilon \cdot (\mathbf{k} - x\mathbf{q}_1)}{(\mathbf{k} - x\mathbf{q}_1)^2 + m_g^2(1-x+x^2)} e^{\frac{i}{2\omega}(\mathbf{k}^2 + \frac{x}{1-x}(\mathbf{k}-\mathbf{q}_1)^2 + \frac{m_g^2(1-x+x^2)}{1-x})(z_1-z_0)}$$

$$M_{1,0,0} = J_a(p+k)e^{i(p+k)x_0}(-i)(1-x+x^2)(T^{a_1} T^c)_{da} T_{a_1} \int \frac{d^2 \mathbf{q}_1}{(2\pi)^2} v(0, \mathbf{q}_1) e^{-i\mathbf{q}_1 \cdot \mathbf{b}_1} \times (2ig_s) \frac{\epsilon \cdot \mathbf{k}}{k^2 + \chi} \left(e^{\frac{i}{2\omega}(\mathbf{k}^2 + \frac{x}{1-x}(\mathbf{k}-\mathbf{q}_1)^2 + \frac{\chi}{1-x})(z_1-z_0)} - e^{-\frac{i}{2\omega} \frac{x}{1-x}(\mathbf{k}^2 - (\mathbf{k}-\mathbf{q}_1)^2)(z_1-z_0)} \right)$$

$$M_{1,0,1} = J_a(p+k)e^{i(p+k)x_0}(-i)(1-x+x^2)[T^c, T^{a_1}]_{da} T_{a_1} \int \frac{d^2 \mathbf{q}_1}{(2\pi)^2} v(0, \mathbf{q}_1) e^{-i\mathbf{q}_1 \cdot \mathbf{b}_1} \times (2ig_s) \frac{\epsilon \cdot (\mathbf{k} - \mathbf{q}_1)}{(\mathbf{k} - \mathbf{q}_1)^2 + \chi} \left(e^{\frac{i}{2\omega}(\mathbf{k}^2 + \frac{x}{1-x}(\mathbf{k}-\mathbf{q}_1)^2 + \frac{\chi}{1-x})(z_1-z_0)} - e^{\frac{i}{2\omega}(\mathbf{k}^2 - (\mathbf{k}-\mathbf{q}_1)^2)(z_1-z_0)} \right)$$

One interaction with QGP medium

Symmetric
under the
exchange of
radiated (**k**)
and final
gluon (**p**).

**Recovers *sg* result
for $x \ll 1$.**

Calculations beyond soft-gluon approximation

$$M_{2,2,0}^c = -J_a(p+k)e^{i(p+k)x_0}(T^c T^{a_2} T^{a_1})_{da} T_{a_2} T_{a_1} (1-x+x^2)(-i) \int \frac{d^2 \mathbf{q}_1}{(2\pi)^2} (-i) \int \frac{d^2 \mathbf{q}_2}{(2\pi)^2} v(0, \mathbf{q}_1) v(0, \mathbf{q}_2) e^{-i(\mathbf{q}_1 + \mathbf{q}_2) \cdot \mathbf{b}_1} \\ \times \frac{1}{2} (2ig_s) \frac{\epsilon \cdot (\mathbf{k} - x(\mathbf{q}_1 + \mathbf{q}_2))}{(\mathbf{k} - x(\mathbf{q}_1 + \mathbf{q}_2))^2 + \chi} e^{\frac{i}{2\omega}(\mathbf{k}^2 + \frac{x}{1-x}(\mathbf{k} - \mathbf{q}_1 - \mathbf{q}_2)^2 + \frac{\chi}{1-x})(z_1 - z_0)}$$

Two interactions with QGP medium

$$M_{2,0,3}^c = J_a(p+k)e^{i(p+k)x_0}[[T^c, T^{a_2}], T^{a_1}]_{da} T_{a_2} T_{a_1} (1-x+x^2)(-i) \int \frac{d^2 \mathbf{q}_1}{(2\pi)^2} (-i) \int \frac{d^2 \mathbf{q}_2}{(2\pi)^2} v(0, \mathbf{q}_1) v(0, \mathbf{q}_2) e^{-i(\mathbf{q}_1 + \mathbf{q}_2) \cdot \mathbf{b}_1} \\ \times \frac{1}{2} (2ig_s) \frac{\epsilon \cdot (\mathbf{k} - \mathbf{q}_1 - \mathbf{q}_2)}{(\mathbf{k} - \mathbf{q}_1 - \mathbf{q}_2)^2 + \chi} \left(e^{\frac{i}{2\omega}(\mathbf{k}^2 + \frac{x}{1-x}(\mathbf{k} - \mathbf{q}_1 - \mathbf{q}_2)^2 + \frac{\chi}{1-x})(z_1 - z_0)} - e^{\frac{i}{2\omega}(\mathbf{k}^2 - (\mathbf{k} - \mathbf{q}_1 - \mathbf{q}_2)^2)(z_1 - z_0)} \right)$$

$$M_{2,0,0}^c = J_a(p+k)e^{i(p+k)x_0}(T^{a_2} T^{a_1} T^c)_{da} T_{a_2} T_{a_1} (1-x+x^2)(-i) \int \frac{d^2 \mathbf{q}_1}{(2\pi)^2} (-i) \int \frac{d^2 \mathbf{q}_2}{(2\pi)^2} v(0, \mathbf{q}_1) v(0, \mathbf{q}_2) e^{-i(\mathbf{q}_1 + \mathbf{q}_2) \cdot \mathbf{b}_1} \\ \times \frac{1}{2} (2ig_s) \frac{\epsilon \cdot \mathbf{k}}{\mathbf{k}^2 + \chi} \left(e^{\frac{i}{2\omega}(\mathbf{k}^2 + \frac{x}{1-x}(\mathbf{k} - \mathbf{q}_1 - \mathbf{q}_2)^2 + \frac{\chi}{1-x})(z_1 - z_0)} - e^{\frac{i}{2\omega} \frac{x}{1-x} ((\mathbf{k} - \mathbf{q}_1 - \mathbf{q}_2)^2 - \mathbf{k}^2)(z_1 - z_0)} \right)$$

$$M_{2,0,1}^c = J_a(p+k)e^{i(p+k)x_0}(T^{a_2} [T^c, T^{a_1}])_{da} T_{a_2} T_{a_1} (1-x+x^2)(-i) \int \frac{d^2 \mathbf{q}_1}{(2\pi)^2} (-i) \int \frac{d^2 \mathbf{q}_2}{(2\pi)^2} v(0, \mathbf{q}_1) v(0, \mathbf{q}_2) e^{-i(\mathbf{q}_1 + \mathbf{q}_2) \cdot \mathbf{b}_1} \\ \times (2ig_s) \frac{\epsilon \cdot (\mathbf{k} - \mathbf{q}_1)}{(\mathbf{k} - \mathbf{q}_1)^2 + \chi} \left(e^{\frac{i}{2\omega}(\mathbf{k}^2 + \frac{x}{1-x}(\mathbf{k} - \mathbf{q}_1 - \mathbf{q}_2)^2 + \frac{\chi}{1-x})(z_1 - z_0)} - e^{\frac{i}{2\omega}(\mathbf{k}^2 - \frac{(\mathbf{k} - \mathbf{q}_1)^2}{1-x} + \frac{x}{1-x}(\mathbf{k} - \mathbf{q}_1 - \mathbf{q}_2)^2)(z_1 - z_0)} \right)$$

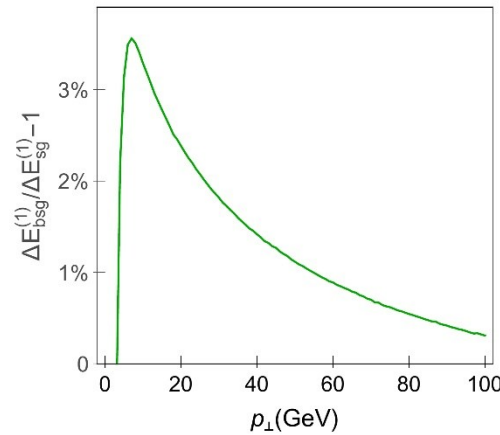
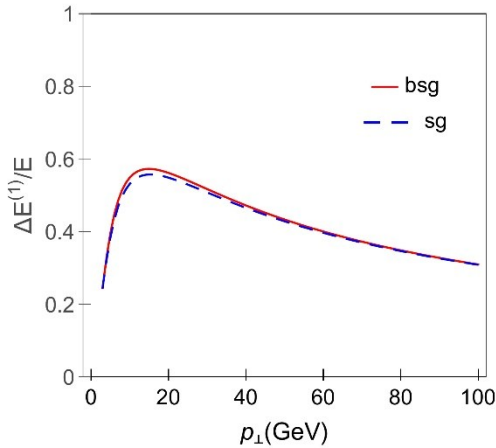
$$M_{2,0,2}^c = J_a(p+k)e^{i(p+k)x_0}(T^{a_1} [T^c, T^{a_2}])_{da} T_{a_2} T_{a_1} (1-x+x^2)(-i) \int \frac{d^2 \mathbf{q}_1}{(2\pi)^2} (-i) \int \frac{d^2 \mathbf{q}_2}{(2\pi)^2} v(0, \mathbf{q}_1) v(0, \mathbf{q}_2) e^{-i(\mathbf{q}_1 + \mathbf{q}_2) \cdot \mathbf{b}_1} \\ \times (2ig_s) \frac{\epsilon \cdot (\mathbf{k} - \mathbf{q}_2)}{(\mathbf{k} - \mathbf{q}_2)^2 + \chi} \left(e^{\frac{i}{2\omega}(\mathbf{k}^2 + \frac{x}{1-x}(\mathbf{k} - \mathbf{q}_1 - \mathbf{q}_2)^2 + \frac{\chi}{1-x})(z_1 - z_0)} - e^{\frac{i}{2\omega}(\mathbf{k}^2 - \frac{(\mathbf{k} - \mathbf{q}_2)^2}{1-x} + \frac{x}{1-x}(\mathbf{k} - \mathbf{q}_1 - \mathbf{q}_2)^2)(z_1 - z_0)} \right)$$

Symmetric under the exchange of **k** and **p** gluons.

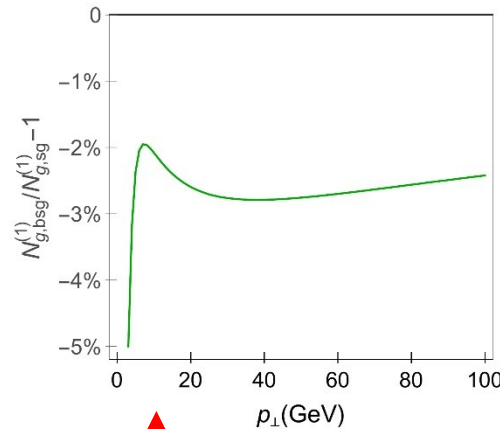
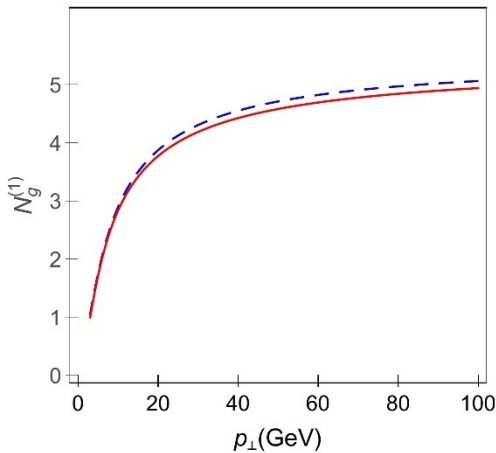
Recovers *sg* result for $x \ll 1$.

Two negligible amplitudes are omitted.

Effect of relaxing *sga* on numerical predictions



Finite x slightly **increases** fractional radiative energy loss up to $\approx 3\%$ compared to ***sg***.



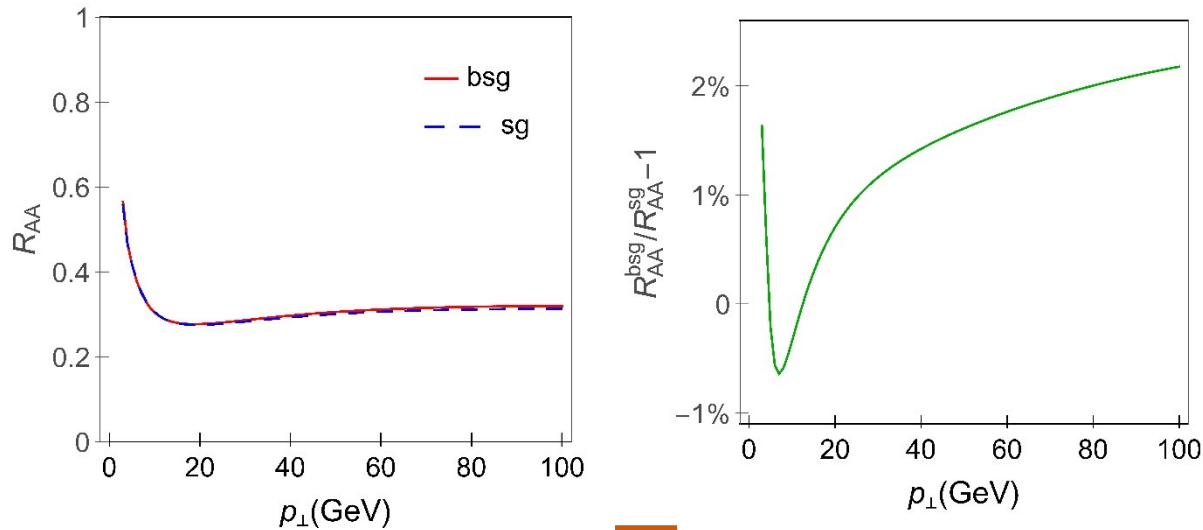
Finite x slightly **decreases** number of radiated gluons $\approx -2\%$ compared to ***sg***.



$\approx 10 \text{ GeV}$

Effect on $\Delta E^{(1)}/E$ and $N_g^{(1)}$ is **very small** and of an **opposite sign!**

Effect of relaxing *sga* on R_{AA}

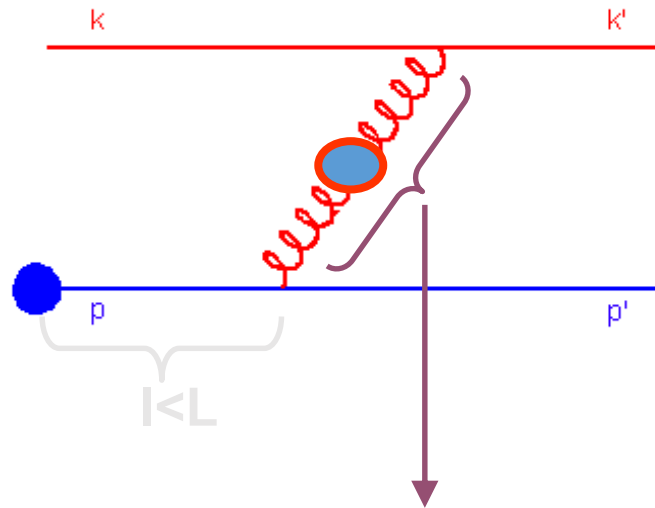


R_{AA} **negligibly**
affected by this relaxation!



Why is R_{AA} barely affected by this relaxation?

Collisional energy loss in a finite size QCD medium



The effective gluon propagator:

$$D^{\mu\nu}(\omega, \vec{q}) = -P^{\mu\nu} \Delta_T(\omega, \vec{q}) - Q^{\mu\nu} \Delta_L(\omega, \vec{q})$$

1-HTL gluon propagator:

$$iD^{\mu\nu}(l) = \frac{P^{\mu\nu}(l)}{l^2 - \Pi_T(l)} + \frac{Q^{\mu\nu}(l)}{l^2 - \Pi_L(l)}$$



Cut 1-HTL gluon propagator:

$$D_{\mu\nu}^>(l) = -(1+f(l_0)) \left(P_{\mu\nu}(l) \rho_T(l) + Q_{\mu\nu}(l) \rho_L(l) \right),$$

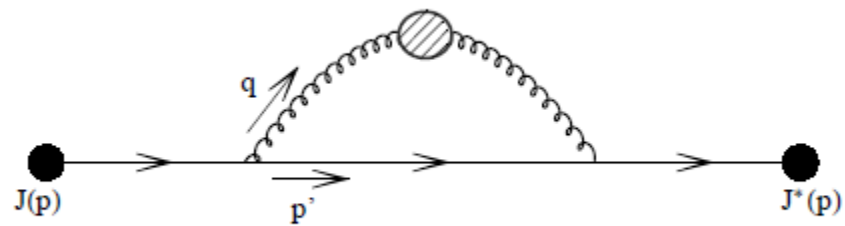
$$\rho_{L,T}(l) = \underbrace{2\pi \delta(l^2 - \Pi_{T,L}(l))}_{\text{Radiated gluon}} - 2 \underbrace{\text{Im} \left(\frac{1}{l^2 - \Pi_{T,L}(l)} \right) \theta(1 - \frac{l_0^2}{\vec{l}^2})}_{\text{Exchanged gluon}}$$

For **radiated gluon**, cut 1-HTL gluon propagator can be **simplified** to
(M.D. and M. Gyulassy, PRC 68, 034914 (2003)).

$$D_{\mu\nu}^>(k) \approx -2\pi \frac{P_{\mu\nu}(k)}{2\omega} \delta(k_0 - \omega) \quad \omega \approx \sqrt{\vec{k}^2 + m_g^2}; \quad m_g \approx \mu/\sqrt{2}$$

For **exchanged gluon**, cut 1-HTL gluon propagator cannot be simplified, since **both transverse** (magnetic) **and longitudinal** (electric) contributions will prove to be **important**.

$$D_{\mu\nu}^>(q) = \theta(1 - \frac{q_0^2}{\vec{q}^2}) (1 + f(q_0)) 2 \text{Im} \left(\frac{P_{\mu\nu}(q)}{q^2 - \Pi_T(q)} + \frac{Q_{\mu\nu}(q)}{q^2 - \Pi_L(q)} \right)$$



One Hard Thermal Loop (HTL) diagram.

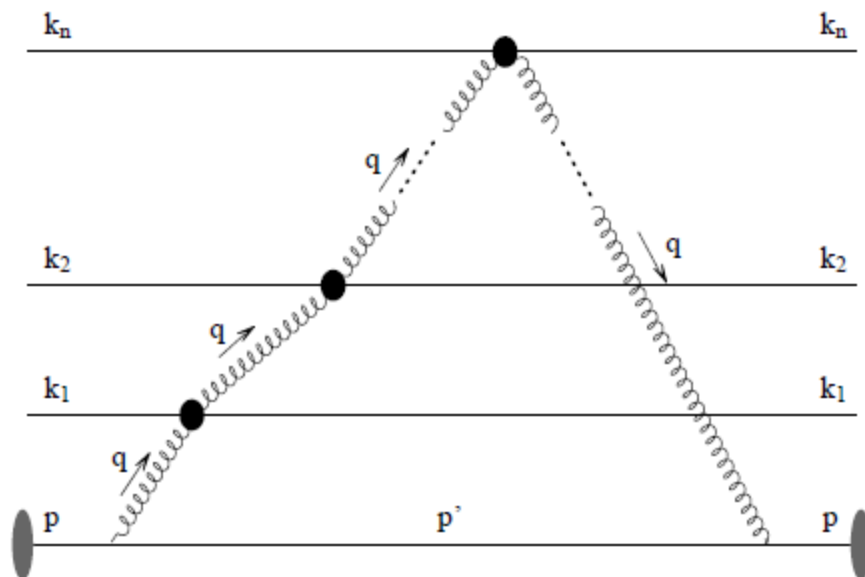
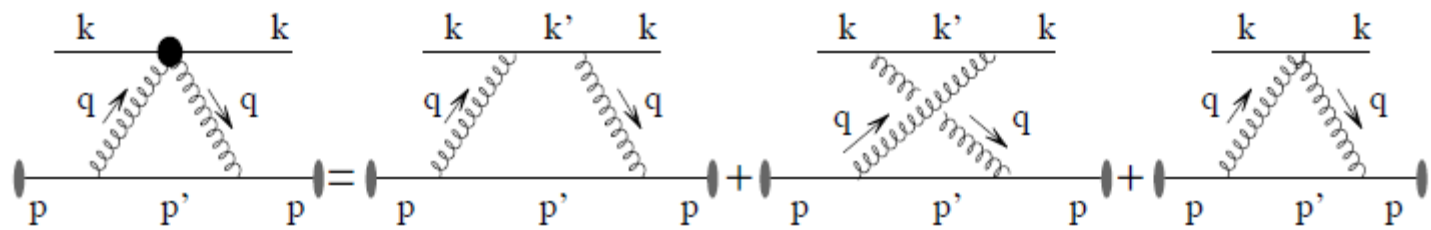
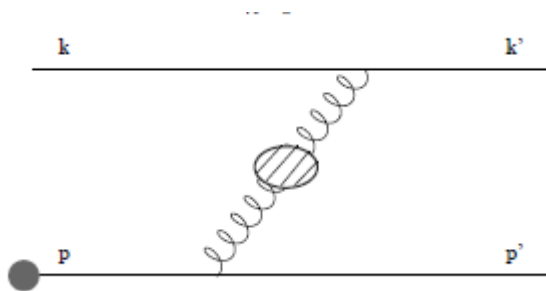


Diagram M_n

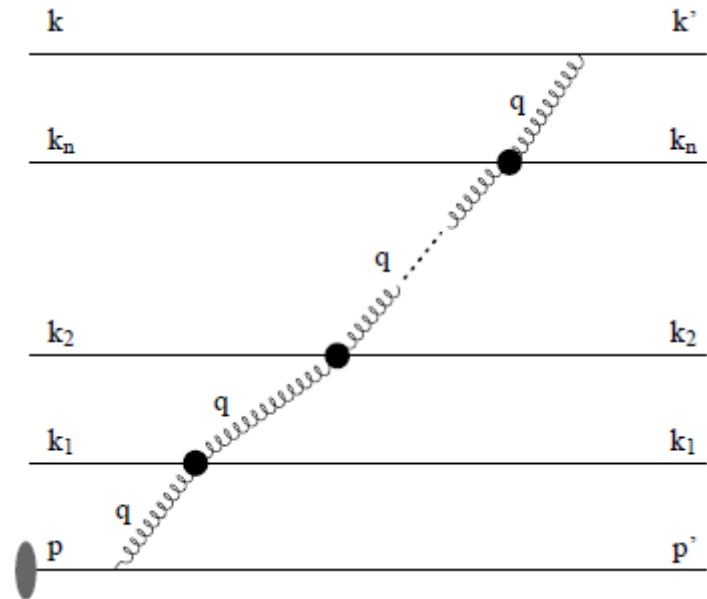
$$\begin{array}{c}
 k_i \\
 \uparrow q \\
 \text{---} \bullet \text{---} k_i \\
 \downarrow q
 \end{array}
 =
 \begin{array}{c}
 k_i \\
 \uparrow q \\
 \text{---} \bullet \text{---} k_i + q \\
 \downarrow q
 \end{array}
 +
 \begin{array}{c}
 k_i \\
 \uparrow q \\
 \text{---} \bullet \text{---} k_i - q \\
 \downarrow q
 \end{array}
 +
 \begin{array}{c}
 k_i \\
 \uparrow q \\
 \text{---} \bullet \text{---} k_i \\
 \downarrow q
 \end{array}$$



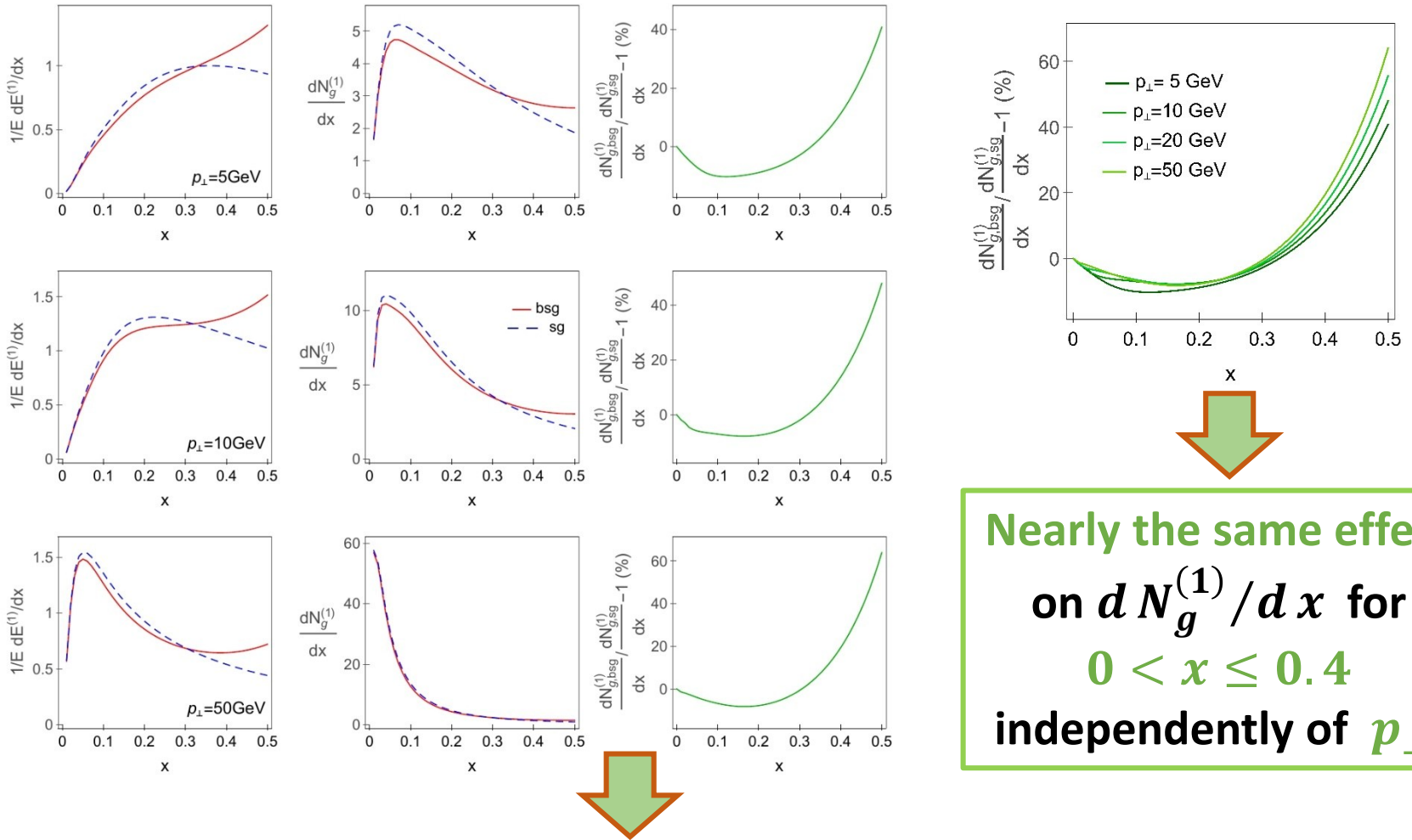
Collisional energy loss



$$= \sum_{n=0}^{\infty}$$



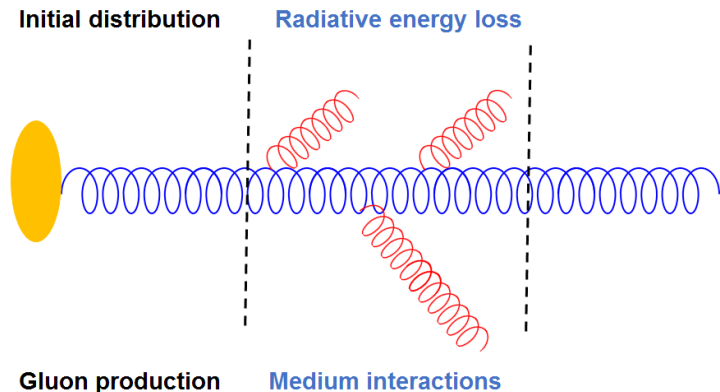
Effect of relaxing *sga* on numerical predictions



Nearly the same effect
on $dN_g^{(1)}/dx$ for
 $0 < x \leq 0.4$
independently of p_{\perp} .

The effect on $dE^{(1)}/dx$ and $dN_g^{(1)}/dx$ is **small** for $x \leq 0.4$,
while **enhances** to a notable value with increasing x above
the “cross-over” point $x \approx 0.3$.

Computational formalism for bare gluon suppression



1. Initial gluon p_{\perp} spectrum
2. Radiative energy loss

- **Gluon production**

(Z.B. Kang, I. Vitev and H. Xing, PLB 718:482 (2012); R. Sharma, I. Vitev and B.W. Zhang, PRC 80:054902 (2009))

- **Radiative energy loss in finite size static QGP medium *beyond soft gluon approximation***

(B. Blagojevic, M. Djordjevic and M. Djordjevic, PRC 99, 024901, (2019))

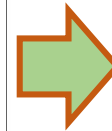
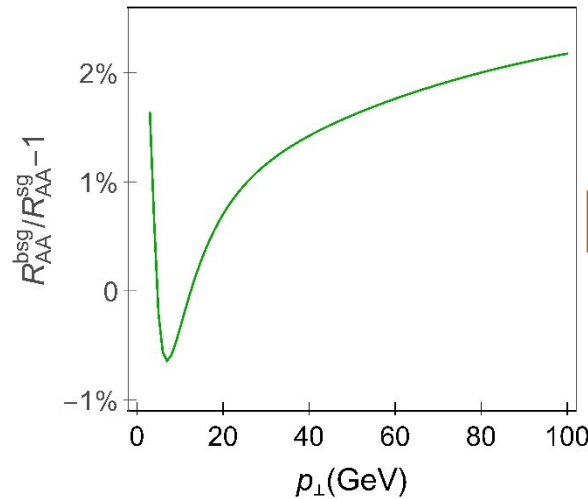
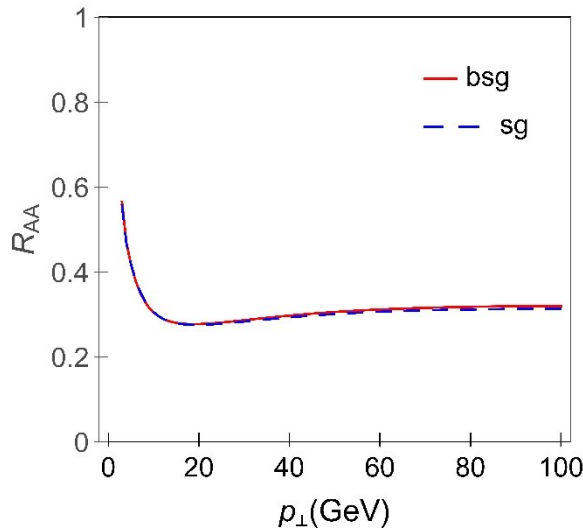
- **Multi-gluon fluctuations**

(M. Gyulassy, P. Levai and I. Vitev, PLB 538:282 (2002))

- **Path-length fluctuations**

(S. Wicks, W. Horowitz, M. Djordjevic and M. Gyulassy, NPA 784:426 (2007); A. Dainese, EPJ C 33:495 (2004))

Effect of relaxing *sga* on R_{AA}

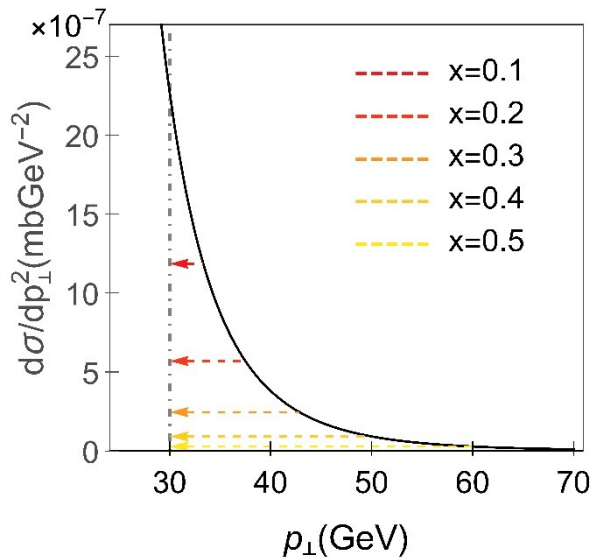
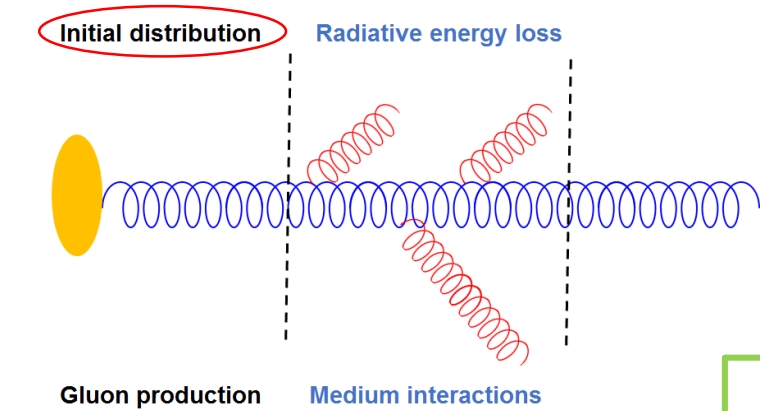


R_{AA}
negligibly affected
by this relaxation!



How the large differential variables
discrepancies between *bsg* and *sg* cases at $x >$
0.4 do not influence R_{AA} ?

Explanation of negligible effect on R_{AA}



Due to sharply decreasing initial gluon p_{\perp} distribution, the $x \leq 0.4$ is the most relevant region for distinguishing bsg from $sg R_{AA}$.

In this region bsg and $sg \frac{dN_g^{(1)}}{dx}$ and $\frac{1}{E} \frac{dE^{(1)}}{dx}$ are within 10%.

Intuitively explains insignificant finite x effect on R_{AA} .

Relaxing the soft-gluon approximation

❑ Beyond soft-gluon approximation (**bsg**) in DGLV: **x finite**

✓ DGLV formalism assumes:

Finite size (L) optically thin QGP medium

Static scattering centers $V_n = 2\pi\delta(q_n^0)v(\vec{q}_n)e^{-i\vec{q}_n\cdot\vec{x}_n}T_{a_n}(R) \otimes T_{a_n}(n)$

$$v(\vec{q}_n) = \frac{4\pi\alpha_s}{\vec{q}_n^2 + \mu^2}$$

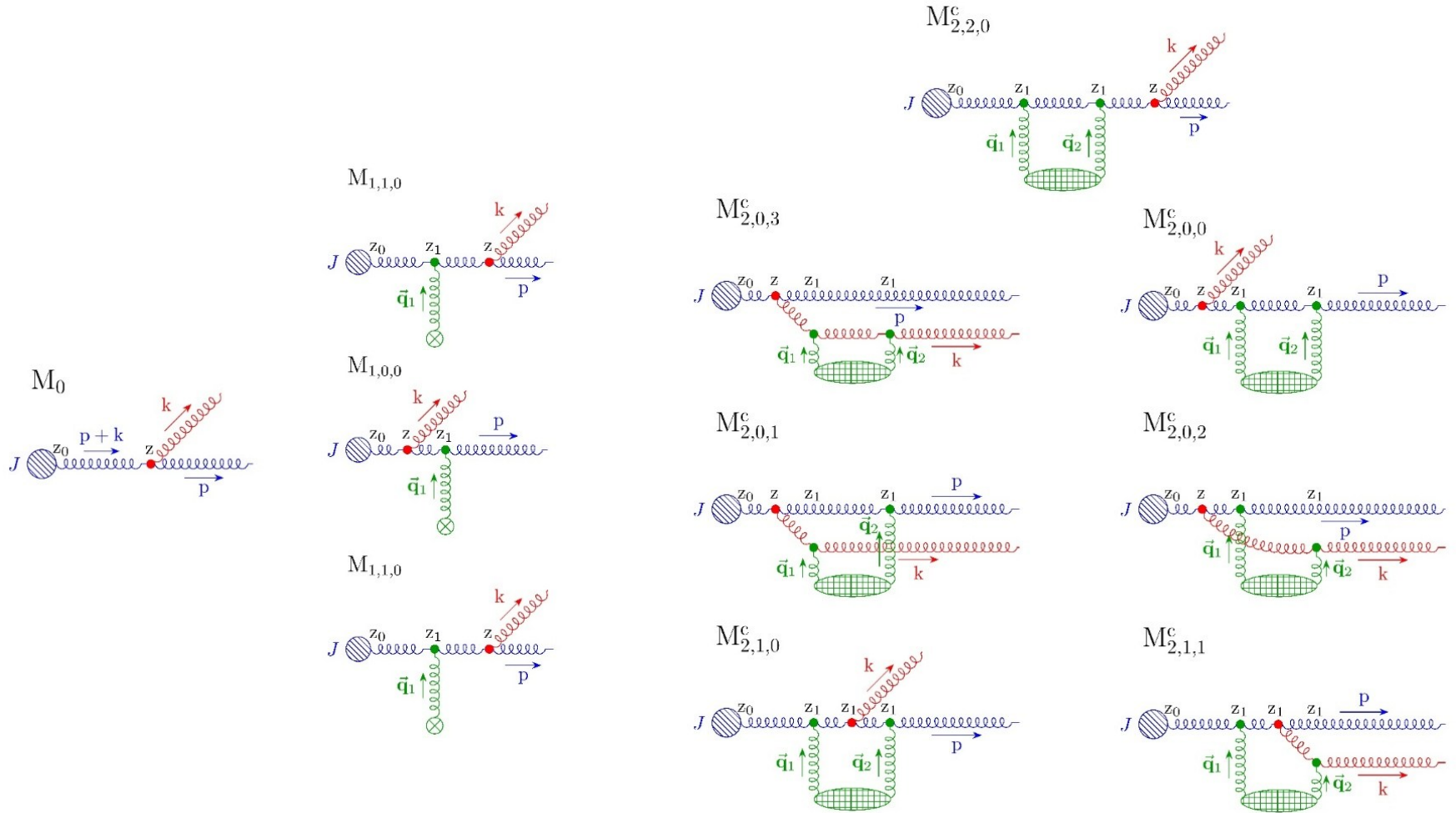
Gluons as transversely polarized partons with effective mass

$$m_g = \mu/\sqrt{2}$$

(M. Djordjevic and M. Gyulassy, PRC 68:034914 (2003))

(B. Blagojevic, M. Djordjevic and M. Djordjevic, PRC 99, 024901, (2019))

Calculations beyond soft-gluon approximation



Calculations beyond soft-gluon approximation

$$\frac{xd^3N_g^{(0)}}{dxdk^2} = \frac{\alpha_s}{\pi} \frac{C_2(G) k^2}{(k^2 + m_g^2(1-x+x^2))^2} \times \frac{(1-x+x^2)^2}{1-x}.$$



**Reduces to well-known
Altarelli-Parisi (G.
Altarelli and G. Parisi, NPB
126:298 (1977)) result in
massless case.**

Single gluon radiation spectrum beyond soft-gluon approximation:

$$\begin{aligned} \frac{dN_g^{(1)}}{dx} = & \frac{C_2(G)\alpha_s}{\pi} \frac{L}{\lambda} \frac{(1-x+x^2)^2}{x(1-x)} \int \frac{d^2\mathbf{q}_1}{\pi} \frac{\mu^2}{(\mathbf{q}_1^2 + \mu^2)^2} \int dk^2 \\ & \times \left\{ \frac{(\mathbf{k} - \mathbf{q}_1)^2 + \chi}{\left(\frac{4x(1-x)E}{L}\right)^2 + ((\mathbf{k} - \mathbf{q}_1)^2 + \chi)^2} \left(2 \frac{(\mathbf{k} - \mathbf{q}_1)^2}{(\mathbf{k} - \mathbf{q}_1)^2 + \chi} - \frac{\mathbf{k} \cdot (\mathbf{k} - \mathbf{q}_1)}{k^2 + \chi} - \frac{(\mathbf{k} - \mathbf{q}_1) \cdot (\mathbf{k} - x\mathbf{q}_1)}{(\mathbf{k} - x\mathbf{q}_1)^2 + \chi} \right) \right. \\ & \left. + \frac{k^2 + \chi}{\left(\frac{4x(1-x)E}{L}\right)^2 + (k^2 + \chi)^2} \left(\frac{k^2}{k^2 + \chi} - \frac{\mathbf{k} \cdot (\mathbf{k} - x\mathbf{q}_1)}{(\mathbf{k} - x\mathbf{q}_1)^2 + \chi} \right) + \left(\frac{(\mathbf{k} - x\mathbf{q}_1)^2}{((\mathbf{k} - x\mathbf{q}_1)^2 + \chi)^2} - \frac{k^2}{(k^2 + \chi)^2} \right) \right\} \end{aligned}$$



(B. Blagojevic, M. Djordjevic and M.
Djordjevic, PRC 99, 024901, (2019))

**Introduction of effective gluon
mass *bsg* radiative energy loss
for the first time!**

Calculations beyond soft-gluon approximation

Longitudinal initial gluon direction:

No interactions with QGP medium (M_0)	One interaction with QGP medium (M_1)	Two interactions with QGP medium (M_2)
$p + k = [E^+, E^-, \mathbf{0}]$	$p + k - q_1 = [E^+ - q_{1z}, E^- + q_{1z}, \mathbf{0}]$	$p + k - q_1 - q_2$
$k = [xE^+, \frac{\mathbf{k}^2 + m_g^2}{xE^+}, \mathbf{k}] \quad p = [(1-x)E^+, \frac{\mathbf{p}^2 + m_g^2}{(1-x)E^+}, \mathbf{p}]$		
Transverse momenta: $\mathbf{p} + \mathbf{k} = \mathbf{0}$	Transverse momenta: $\mathbf{p} + \mathbf{k} \neq \mathbf{0}$ <div>Consistent with longitudinal propagation of initial particle!</div>	
Transverse gluon polarization: $n^\mu = [0, 2, 0]$		
$\epsilon(k) \cdot k = 0,$ $\epsilon(p) \cdot p = 0,$	$\epsilon(k) \cdot n = 0,$ $\epsilon(p) \cdot n = 0,$	$\epsilon(k)^2 = -1,$ $\epsilon(p)^2 = -1,$
$\epsilon(p+k) \cdot (p+k) = 0,$ $\epsilon(p+k)^2 = -1.$		
$\epsilon_i(k) = [0, \frac{2\epsilon_i \cdot \mathbf{k}}{xE^+}, \epsilon_i],$ $\epsilon_i(p+k) = [0, 0, \epsilon_i],$ $\epsilon_i(p) = [0, \frac{2\epsilon_i \cdot \mathbf{p}}{(1-x)E^+}, \epsilon_i],$		

Calculations beyond soft-gluon approximation

$$d^3 N_g^{(1)} d^3 N_J = \left(\frac{1}{d_T} \text{Tr} \langle |M_1|^2 \rangle + \frac{2}{d_T} \text{Re} \text{Tr} \langle M_2 M_0^* \rangle \right) \frac{d^3 \vec{p}}{(2\pi)^3 2p^0} \frac{d^3 \vec{k}}{(2\pi)^3 2\omega}$$

New!

$$d^3 N_J = d_G |J(p+k)|^2 \frac{d^3 \vec{p}_J}{(2\pi)^3 2E_J}$$

$$\frac{d^3 \vec{p}}{(2\pi)^3 2p^0} \frac{d^3 \vec{k}}{(2\pi)^3 2\omega} = \frac{d^3 \vec{p}_J}{(2\pi)^3 2E_J} \frac{dx d^2 \mathbf{k}}{(2\pi)^3 2x(1-x)}$$

$$\begin{aligned} \frac{x d^3 N_g^{(0)}}{dx d\mathbf{k}^2} &= \frac{\alpha_s}{\pi} \frac{C_2(G) \mathbf{k}^2}{(\mathbf{k}^2 + m_g^2 (1-x+x^2))^2} \\ &\times \frac{(1-x+x^2)^2}{1-x}. \end{aligned}$$

$$\begin{aligned} \frac{dN_g^{(1)}}{dx} &= \frac{C_2(G) \alpha_s}{\pi} \frac{L}{\lambda} \frac{(1-x+x^2)^2}{x(1-x)} \int \frac{d^2 \mathbf{q}_1}{\pi} \frac{\mu^2}{(\mathbf{q}_1^2 + \mu^2)^2} \int d\mathbf{k}^2 \\ &\times \left\{ \frac{(\mathbf{k} - \mathbf{q}_1)^2 + \chi}{\left(\frac{4x(1-x)E}{L}\right)^2 + ((\mathbf{k} - \mathbf{q}_1)^2 + \chi)^2} \left(2 \frac{(\mathbf{k} - \mathbf{q}_1)^2}{(\mathbf{k} - \mathbf{q}_1)^2 + \chi} - \frac{\mathbf{k} \cdot (\mathbf{k} - \mathbf{q}_1)}{\mathbf{k}^2 + \chi} - \frac{(\mathbf{k} - \mathbf{q}_1) \cdot (\mathbf{k} - x\mathbf{q}_1)}{(\mathbf{k} - x\mathbf{q}_1)^2 + \chi} \right) \right. \\ &\left. + \frac{\mathbf{k}^2 + \chi}{\left(\frac{4x(1-x)E}{L}\right)^2 + (\mathbf{k}^2 + \chi)^2} \left(\frac{\mathbf{k}^2}{\mathbf{k}^2 + \chi} - \frac{\mathbf{k} \cdot (\mathbf{k} - x\mathbf{q}_1)}{(\mathbf{k} - x\mathbf{q}_1)^2 + \chi} \right) + \left(\frac{(\mathbf{k} - x\mathbf{q}_1)^2}{((\mathbf{k} - x\mathbf{q}_1)^2 + \chi)^2} - \frac{\mathbf{k}^2}{(\mathbf{k}^2 + \chi)^2} \right) \right\} \end{aligned}$$

Beyond soft-gluon analytical results

- The *bsg* single gluon radiation spectrum $\frac{dN_g^{(1)}}{dx}$ is:
 - Is more complicated than in soft-gluon (*sg*) case.
 - Recovers *sg* result for $x \ll 1$.
 - Is *symmetric* under the exchange of radiated (*k*) and final gluon (*p*).

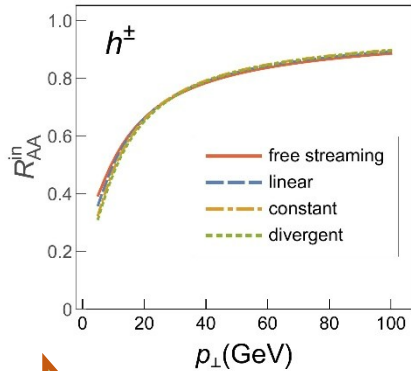
Generalization on dynamical medium

- Implicitly suggested by robust agreement of our R_{AA} predictions with experimental data
- Only $f(k, q, x)$ depends on x
- $f(k, q, x)$ in soft-gluon approximation is the same in static and in dynamical case



We expect dynamical $f(k, q, x)$ to be modified in the similar manner to the static (DGLV) case.

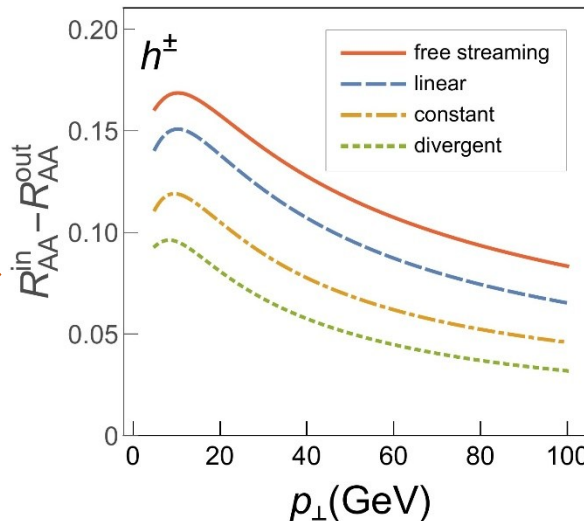
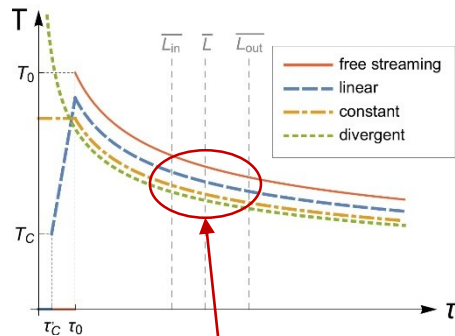
Is IS responsible for high- p_{\perp} v_2 discrepancies?



No effect on R_{AA}^{in} .

Only R_{AA}^{out} differences are responsible for v_2 discrepancies.

$$-R_{AA} \sim \bar{T}$$



The same curve ordering as modified T profiles in $(\bar{L}_{in}, \bar{L}_{out})$ region.

Only this region contributes to R_{AA}^{out} differences.

v_2 differences originate from interactions of high- p_{\perp} parton with *thermalized* QGP, and *not the initial stages*!

Energy losses in DREENA-B framework

Radiative part:

$$\frac{dN_{rad}}{dx d\tau} = \frac{C_2(G)C_R}{\pi} \frac{1}{x} \int \frac{d^2\mathbf{q}}{\pi} \frac{d^2\mathbf{k}}{\pi} \frac{\mu_E^2(T) - \mu_M^2(T)}{[\mathbf{q}^2 + \mu_E^2(T)][\mathbf{q}^2 + \mu_M^2(T)]} T\alpha_s(ET)\alpha_s\left(\frac{\mathbf{k}^2 + \chi(T)}{x}\right) \\ \times \left[1 - \cos\left(\frac{(\mathbf{k} + \mathbf{q})^2 + \chi(T)}{xE^+} \tau\right)\right] \frac{2(\mathbf{k} + \mathbf{q})}{(\mathbf{k} + \mathbf{q})^2 + \chi(T)} \left[\frac{\mathbf{k} + \mathbf{q}}{(\mathbf{k} + \mathbf{q})^2 + \chi(T)} - \frac{\mathbf{k}}{\mathbf{k}^2 + \chi(T)}\right]$$

$$\chi(T) = M^2 x^2 + m_g^2(T)$$

Collisional part:

$$\frac{dE_{coll}}{d\tau} = \frac{2C_R}{\pi v^2} \alpha_s(ET)\alpha_s(\mu_E^2(T)) \int_0^\infty n_{eq}(|\vec{\mathbf{k}}|, T) d|\vec{\mathbf{k}}| \\ \times \left[\int_0^{|\vec{\mathbf{k}}|/(1+v)} d|\vec{\mathbf{q}}| \int_{-v|\vec{\mathbf{q}}|}^{v|\vec{\mathbf{q}}|} \omega d\omega + \int_{|\vec{\mathbf{k}}|/(1+v)}^{|\vec{\mathbf{q}}|_{max}} d|\vec{\mathbf{q}}| \int_{|\vec{\mathbf{q}}|-2|\vec{\mathbf{k}}|}^{v|\vec{\mathbf{q}}|} \omega d\omega \right] \\ \times \left[|\Delta_L(q, T)|^2 \frac{(2|\vec{\mathbf{k}}| + \omega)^2 - |\vec{\mathbf{q}}|^2}{2} + |\Delta_T(q, T)|^2 \frac{(|\vec{\mathbf{q}}|^2 - \omega^2)((2|\vec{\mathbf{k}}| + \omega)^2 + |\vec{\mathbf{q}}|^2)}{4|\vec{\mathbf{q}}|^4} (v^2|\vec{\mathbf{q}}|^2 - \omega^2) \right]$$

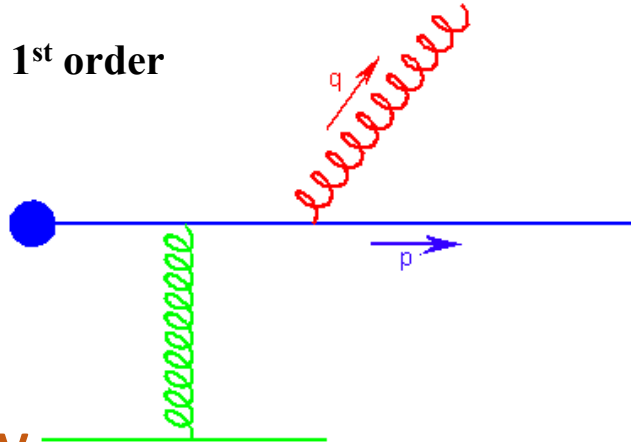
$$n_{eq}(|\vec{\mathbf{k}}|, T) = \frac{N}{e^{|\vec{\mathbf{k}}|/T-1}} + \frac{N_f}{e^{|\vec{\mathbf{k}}|/T+1}}$$

$$\Delta_L^{-1}(T) = \vec{\mathbf{q}}^2 + \mu_E(T)^2 \left(1 + \frac{\omega}{2|\vec{\mathbf{q}}|} \ln \left| \frac{\omega - |\vec{\mathbf{q}}|}{\omega + |\vec{\mathbf{q}}|} \right| \right),$$

$$\Delta_T^{-1}(T) = \omega^2 - \vec{\mathbf{q}}^2 - \frac{\mu_E(T)^2}{2} - \frac{(\omega^2 - \vec{\mathbf{q}}^2)\mu_E(T)^2}{2\vec{\mathbf{q}}^2} \left(1 + \frac{\omega}{2|\vec{\mathbf{q}}|} \ln \left| \frac{\omega - |\vec{\mathbf{q}}|}{\omega + |\vec{\mathbf{q}}|} \right| \right)$$

Radiative energy loss in static medium

1st order



DGLV

Exponential distribution of scatterers

$$\frac{\Delta E_{stat}}{E} = \frac{C_R \alpha_s}{\pi} \frac{L}{\lambda_{stat}} \int dx \int \frac{d^2 q_\perp}{\pi} \frac{\mu_E^2}{(q_\perp^2 + \mu_E^2)^2} \int dk^2 \frac{(\mathbf{k} - \mathbf{q}_\perp)^2 + \chi}{\left(\frac{4xE}{L}\right)^2 + ((\mathbf{k} - \mathbf{q}_\perp)^2 + \chi)^2} \times 2 \left(\frac{(\mathbf{k} - \mathbf{q}_\perp)^2}{(\mathbf{k} - \mathbf{q}_\perp)^2 + \chi} - \frac{\mathbf{k} \cdot (\mathbf{k} - \mathbf{q}_\perp)}{k^2 + \chi} \right)$$

Uniform distribution of scatterers

$$\chi = m_g^2 + x^2 M^2$$

$$\frac{\Delta E_{stat}}{E} = \frac{C_R \alpha_s}{\pi} \frac{L}{\lambda_{stat}} \int dx \int \frac{d^2 q_\perp}{\pi} \frac{\mu_E^2}{(q_\perp^2 + \mu_E^2)^2} \int dk^2 \frac{2}{(\mathbf{k} - \mathbf{q}_\perp)^2 + \chi} \times \left(1 - \frac{\sin\left(\frac{(\mathbf{k} - \mathbf{q}_\perp)^2 + \chi}{2xE} L\right)}{\frac{(\mathbf{k} - \mathbf{q}_\perp)^2 + \chi}{2xE} L} \right) \left(\frac{(\mathbf{k} - \mathbf{q}_\perp)^2}{(\mathbf{k} - \mathbf{q}_\perp)^2 + \chi} - \frac{\mathbf{k} \cdot (\mathbf{k} - \mathbf{q}_\perp)}{k^2 + \chi} \right)$$

Collisional energy loss is considered negligible compared to radiative energy loss!

J.D. Bjorken, FERMILAB-PUB-82-059-THY, 287 (1982),
M.H. Thoma and M. Gyulassy, NPB 351, 491 (1991),
E. Braaten and M.H. Thoma, PRD 44, 1298 (1991); PRD 44, 2625 (1991).

M. Djordjevic and M. Gyulassy NPA 733, 265 (2004).

Static vs. dynamical radiative energy loss (theory)

$$\frac{\Delta E_{rad}}{E} = \frac{C_R \alpha_S}{\pi} \frac{L}{\lambda} \int dx \frac{d^2 k}{\pi} \frac{d^2 q}{\pi} v(\mathbf{q}) \left(1 - \frac{\sin \frac{(\mathbf{k}+\mathbf{q})^2 + \chi L}{xE^+}}{\frac{(\mathbf{k}+\mathbf{q})^2 + \chi L}{xE^+}} \right) \frac{2(\mathbf{k}+\mathbf{q})}{(\mathbf{k}+\mathbf{q})^2 + \chi} \left(\frac{(\mathbf{k}+\mathbf{q})}{(\mathbf{k}+\mathbf{q})^2 + \chi} - \frac{\mathbf{k}}{\mathbf{k}^2 + \chi} \right)$$

Two differences:

$v(\mathbf{q})$ effective cross section:

$$\left[\frac{\mu^2}{(\mathbf{q}^2 + \mu^2)^2} \right]_{stat} \longrightarrow \left[\frac{\mu^2}{\mathbf{q}^2(\mathbf{q}^2 + \mu^2)} \right]_{dyn}$$

λ mean free path:

$$\frac{1}{\lambda_{stat}} \longrightarrow \frac{1}{\lambda_{dyn}} = \frac{1}{c(n_f)} \frac{1}{\lambda_{stat}}$$

Increases energy
loss rate in
dynamical medium

where: $\frac{1}{\lambda_{dyn}} = 3\alpha_S T$

$$c(n_f) = 6 \frac{1.202}{\pi^2} \frac{1 + n_f/4}{1 + n_f/6}$$

Finite magnetic mass effect on R_{AA} (theory)

$$\frac{\Delta E_{rad}}{E} = \frac{C_R \alpha_S}{\pi} \frac{L}{\lambda} \int dx \frac{d^2 k}{\pi} \frac{d^2 q}{\pi} v(\mathbf{q}) \left(1 - \frac{\sin \frac{(\mathbf{k}+\mathbf{q})^2 + \chi}{xE^+} L}{\frac{(\mathbf{k}+\mathbf{q})^2 + \chi}{xE^+} L} \right) \frac{2(\mathbf{k}+\mathbf{q})}{(\mathbf{k}+\mathbf{q})^2 + \chi} \left(\frac{(\mathbf{k}+\mathbf{q})}{(\mathbf{k}+\mathbf{q})^2 + \chi} - \frac{\mathbf{k}}{\mathbf{k}^2 + \chi} \right)$$

Only this part gets modified

$$v(\mathbf{q}) = \frac{\mu_E^2}{\mathbf{q}^2(\mathbf{q}^2 + \mu_E^2)} \longrightarrow \frac{\mu_E^2 - \mu_M^2}{(\mathbf{q}^2 + \mu_E^2)(\mathbf{q}^2 + \mu_M^2)}$$

$$0.4 \leq \frac{\mu_M}{\mu_E} \leq 0.6$$

Causes
suppression
decrease

M.Djordjevic and M. Djordjevic, PLB 709:229 (2012)

Finite magnetic mass effect

$$v(\mathbf{q}) = v_L(\mathbf{q}) - v_T(\mathbf{q})$$
$$v_{L,T}(\mathbf{q}) = \frac{1}{\mathbf{q}^2 + \text{Re}\Pi_{L,T}(\infty)} - \frac{1}{\mathbf{q}^2 + \text{Re}\Pi_{L,T}(0)}$$
$$\text{Re}\Pi_T(\infty) = \text{Re}\Pi_L(\infty) \equiv \mu_{pl}^2$$

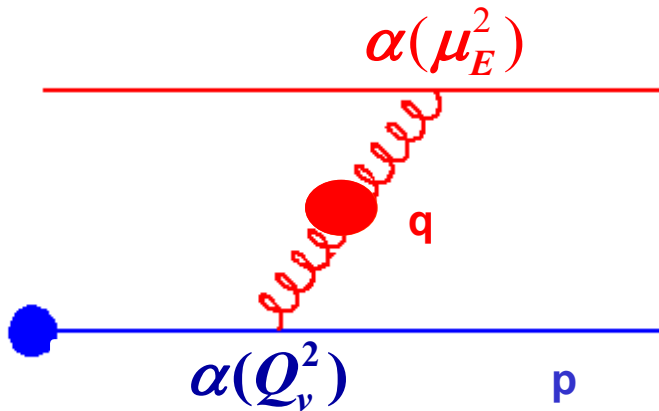
$$\mu_E^2 \equiv \text{Re}\Pi_L(x=0)$$

$$\mu_M^2 \equiv \text{Re}\Pi_T(x=0)$$

Running coupling

Collisional energy loss

S. Peigne, A. Peshier, PRD 77:14017 (2008)



$$\Delta E_{coll} \sim \alpha(Q_v^2) \alpha(\mu_E^2)$$

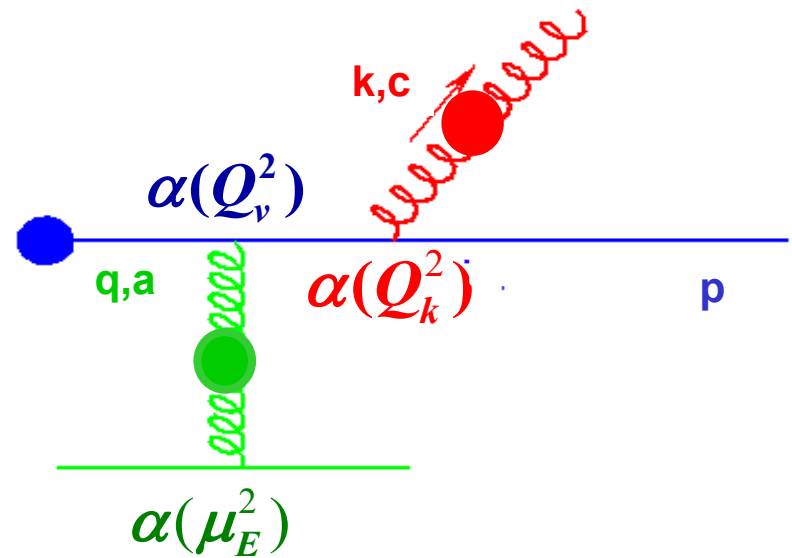
$$\alpha_S(Q^2) = \frac{4\pi}{(11 - 2/3 n_f) \ln(Q^2 / \Lambda_{QCD}^2)}$$

$$\frac{\mu_E^2}{\Lambda_{QCD}^2} \ln \left(\frac{\mu_E^2}{\Lambda_{QCD}^2} \right) = \frac{1 + n_f/6}{11 - 2/3 n_f} \left(\frac{4\pi T}{\Lambda_{QCD}} \right)^2$$

A. Peshier, hep-ph/0601119 (2006)

Radiative energy loss

M. D. and M. Djordjevic, PLB 734 : 286 (2014)



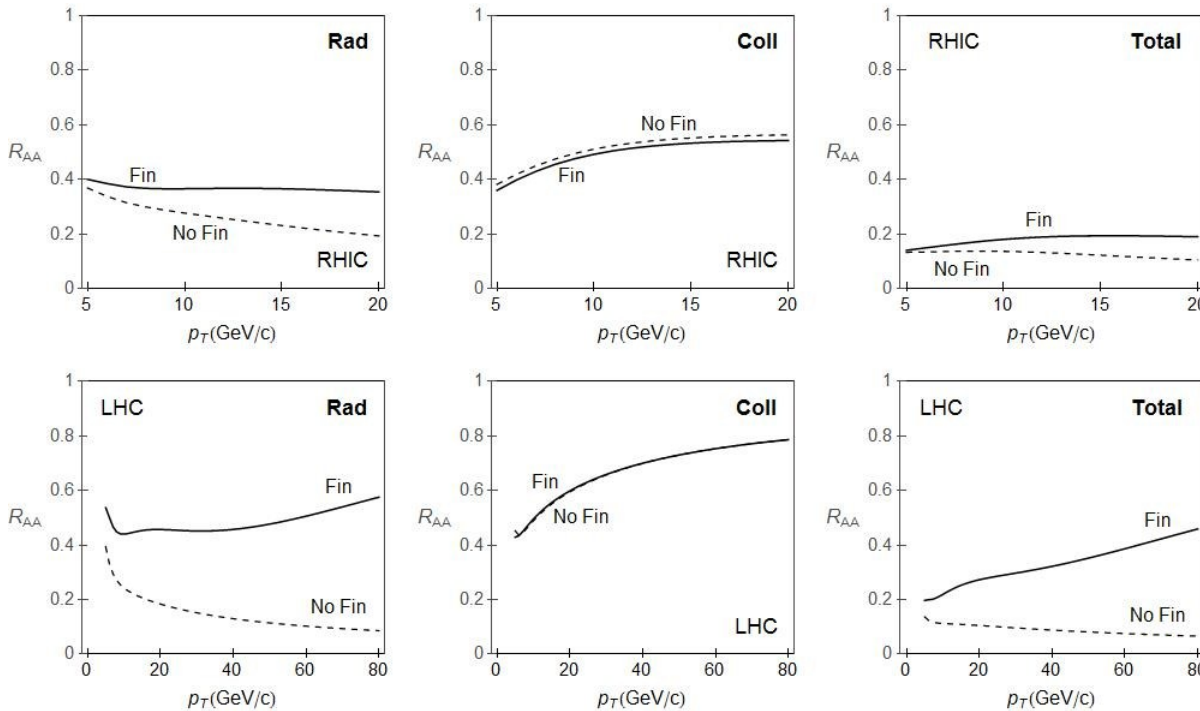
$$\Delta E_{rad} \sim \alpha(Q_k^2) \alpha(Q_v^2) \alpha(\mu_E^2)$$

$$Q_v^2 = ET$$

$$Q_k^2 = \frac{k^2 + M^2 x^2 + m_g^2}{x}$$

Finite size effect on R_{AA}

LPM introduced according to: M.Djordjevic, PRC 80 : 064909 (2009);
M.Djordjevic, PRC 74, : 064907 (2006)

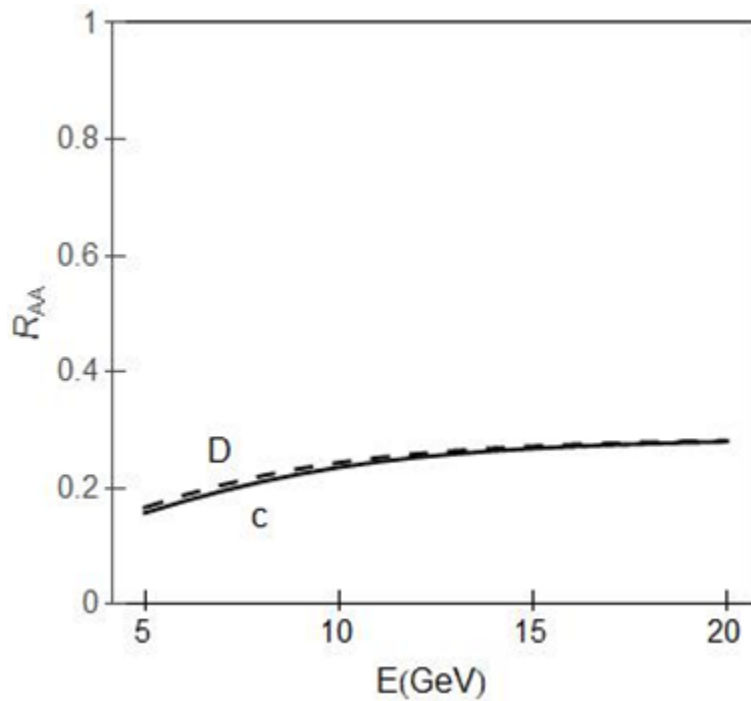


Finite size effect is negligible for collisional, but significant for radiative and total suppression!

Finite size effect is also important!

B.Blagojevic and M. Djordjevic, JPG 42: 075105 (2015)

Charm quark as a clear energy loss probe



**Fragmentation
does not modify
suppression!**



**The clearest
energy loss probe.**

M.Djordjevic and M. Djordjevic, PRL 112:042302 (2014)

$$\Delta E/E \approx \chi \overline{T}^m \overline{L}^n,$$

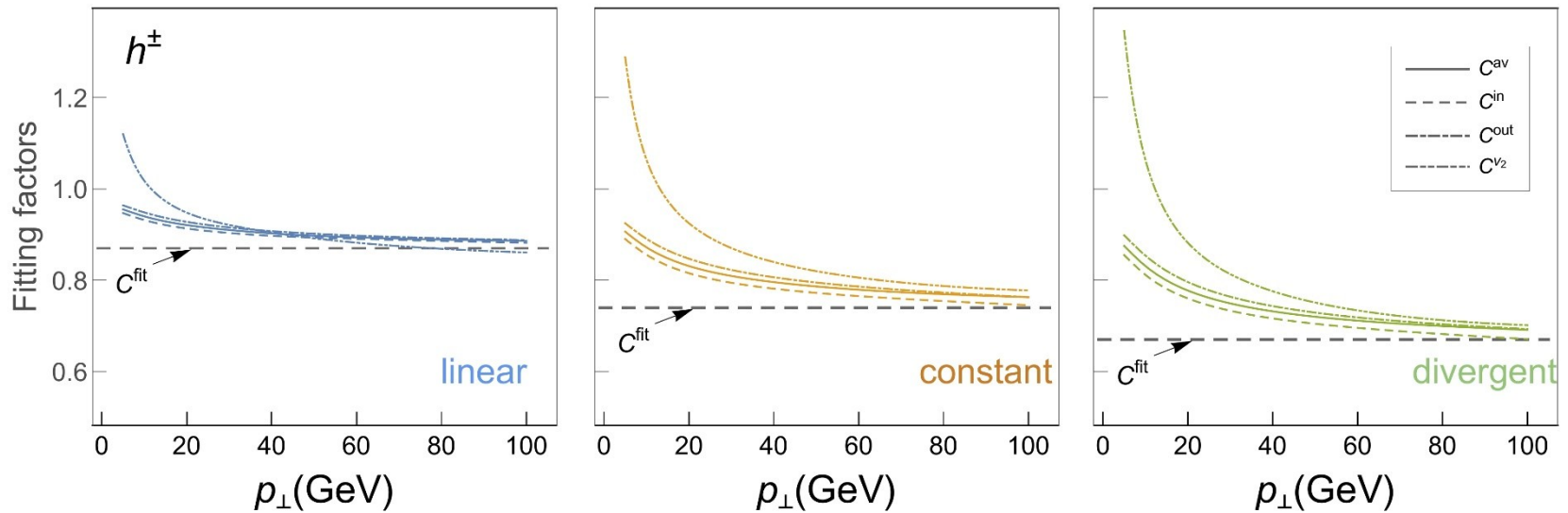
$$R_{AA} \approx 1 - \frac{l-2}{2} \frac{\Delta E}{E} = 1 - \xi \overline{T}^m \overline{L}^n$$

$$R_{AA,i}^{fit} \approx 1 - C_i \xi \overline{T}_i^m \overline{L}_i^n \approx 1 - C_i (1 - R_{AA,i})$$

$$C_i \approx \frac{1 - R_{AA,i}^{fit}}{1 - R_{AA,i}}$$

$$C_i \approx \frac{v_{2,i}^{fit}}{\gamma_{ia} v_{2,a}}$$

Verification of analytic estimate



$$C_i^{in} = \frac{1 - R_{AA,i}^{in,fit}}{1 - R_{AA,i}^{in}}, \quad C_i^{out} = \frac{1 - R_{AA,i}^{out,fit}}{1 - R_{AA,i}^{out}},$$

$$C_i^{av} = \frac{1 - R_{AA,i}^{fit}}{1 - R_{AA,i}}, \quad C_i^{v_2} = \frac{1}{\gamma_i} \frac{v_{2,i}^{fit}}{v_{2,a}},$$

D. Zigic, B. Ilic, M. Djordjevic and M. Djordjevic, arXiv:1908.11866.

(T_{eff}) of 304 MeV for 0-40% centrality 2.76 TeV Pb+Pb

ALICE: NPA 904-905 573c (2013).

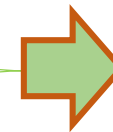


average medium temperature of 348 MeV in most central 5.02 TeV Pb+Pb



$T_C \approx 150 \text{ MeV}$

M. Djordjevic, M. Gyulassy, R. Vogt and S. Wicks, PLB 632, 81 (2006).



$$T_0 \sim (dN_{ch}/dy/A_{\perp})^{1/3}$$

$T_0 = 500 \text{ MeV}$
in most central 5.02 TeV
Pb+Pb

For each
centrality
region.